Available online at www.sciencedirect.com
SCIENCE DIRECT
Journal of Volcanology and Geothermal Research 155 (2006) 18–48
Journal of volcanology and geothermal research
www.elsevier.com/locate/jvolgeores

Dynamical constraints on kimberlite volcanism

R.S.J. Sparks [a,*], L. Baker [a], R.J. Brown [a], M. Field [b], J. Schumacher [a], G. Stripp [a], A Walters [a]

[a] Department of Earth Sciences, University of Bristol, Bristol BS8 1RJ, UK
[b] De Beers MRM R & D Group, Mendip Court, Wells, Somerset, UK

Received 21 March 2005; accepted 6 February 2006
Available online 19 April 2006

Abstract

Kimberlite volcanism involves the ascent of low viscosity (0.1 to 1 Pa s) and volatile-rich (CO_2 and H_2O) ultrabasic magmas from depths of 150 km or greater. Theoretical models and empirical evidence suggest ascent along narrow (~1 m) dykes at speeds in the range >4 to 20 m/s. With typical dyke breadths of 1 to 10 km, magma supply rates are estimated in the range 10^2 to 10^5 m^3/s with eruption durations of many hours to months. Based on observations, theory and experiments we propose a four-stage model for kimberlite eruptions to explain the main geological relationships of kimberlites. In stage I magma reaches the Earth's surface along fissures and erupts explosively due to their high volatile content. The early flow exit conditions are overpressured with choked flow conditions; an exit velocity of ~200 m/s is estimated as representative. Explosive expansion and near surface overpressures initiate crater and pipe formation from the top downwards. In stage II under-pressures (the difference between the lithostatic pressure and pressure of the erupting mixture) develop within the evolving pipe causing rock bursting at depth, undermining overlying rocks and causing down-faulting and crater rim slumping. Rocks falling into the pipe interior are ejected by the strong explosive flows. Stage II is the erosive stage of pipe formation. As the pipe widens and deepens larger under-pressures develop enhancing pipe wall instability. A critical threshold is reached when the exit pressure falls to one atmosphere. As the pipe widens and deepens further the gas exit velocity declines and ejecta becomes trapped within the pipe, initiating stage III. A fluidised bed of pyroclasts develops within the pipe as the eruption wanes to form typical massive volcaniclastic kimberlite. Marginal breccias represent the transition between stages II and III. After the eruption stage IV is a period of hydrothermal metamorphism (principally serpentinisation) and alteration as the pipe cools and meteoric waters infiltrate the hot pipe fill. Following an eruption an open crater can be filled by kimberlite- and country-rock derived sediments, forming the crater-facies.

Keywords: kimberlite; dynamics of eruptions; fluidisation; diamonds

1. Introduction

Kimberlite volcanism has attracted attention because of the deep origin of the magmas and the xenoliths they contain, and their commercial significance as hosts to diamonds. Ideas on the origin of kimberlite pipes have been a long-standing issue invoking some controversy between those who interpret kimberlite geology in terms of explosive degassing of magma (e.g. Dawson, 1971, 1973; Clement, 1975, 1982; Field and Scott Smith, 1999; Skinner and Marsh, 2004) and hydrovolcanic processes (e.g. Lorenz, 1975; Lorenz et al., 1998; Kurszlaukis et al., 1998). There have been several variants of emplacement models of kimberlites with opposed ideas of whether they grow from the top down

* Corresponding author. Tel.: +44 1179 545419.
E-mail address: Steve.Sparks@bristol.ac.uk (R.S.J. Sparks).

0377-0273/$ - see front matter © 2006 Elsevier B.V. All rights reserved.
doi:10.1016/j.jvolgeores.2006.02.010

or bottom up. Fluidisation processes have also been invoked to explain the volcaniclastic rocks that commonly infill kimberlite pipes (Woolsey et al., 1975; Clement, 1982). Kimberlite volcanism also motivated pioneering applications of fluid dynamical models to understand explosive eruptions (McGetchin, 1968; McGetchin and Ullrich, 1973).

Here we approach kimberlite volcanism by applying understanding of volcanic and magmatic processes that have developed over the last three decades to place constraints on kimberlite eruptions. Advances in volcanology have been made through quantitative observations of eruptions and quantitative modelling based on the underlying physics of magma ascent and eruption. Such approaches can be usefully applied to kimberlites, although with recognition that kimberlite magmas have some significant differences (such as very low viscosity and high volatile contents) compared to more common magmas.

Our objective is to develop a conceptual model of kimberlite volcanism based on physical principles and empirical understanding of volcanic processes. We first summarise some of the key geological features of kimberlites; these are the observations that have to be explained and also can provide empirical constraints on what physical models might be viable. This section includes a proposed simple non-genetic classification of kimberlite rock types that avoids the difficulties of using existing nomenclatures that can have strong genetic connotations. The role of secondary alteration processes, in particular pervasive serpentinisation, is discussed since understanding the primary nature of volcaniclastic kimberlitic rocks is dependent on how the textures related to alteration are interpreted. We then consider the physical properties of the erupting magmas and some of the attributes of the eruptions in terms of volume and fluxes of magma, mechanism of forming the pipes and possible external controls such as ground water. Simplified models are presented for the ascent of kimberlite magma, eruptive conditions in explosive eruptions and for the development of a fluidised system in kimberlite pipes. We summarise published information and draw together inferences derived from the observations, physical principles and empirical constraints to propose a model of kimberlite volcanism. The model incorporates some of the earlier concepts, but has new features.

2. Kimberlite geology

In this section we summarise and discuss key features of kimberlite volcanism. Our focus is on those aspects that seem most relevant to understanding and constraining volcanic processes. Some of the features, such as dimensions of kimberlite pipes, can be regarded as uncontentious facts, whereas others are associated with difficulties of interpretation, such as the nature of volcaniclastic and magmatic kimberlite rocks that infill the pipes, the compositions and petrogenesis of the magmas, and the significance of the pervasive serpentinisation.

2.1. Occurrence, distribution and architecture

Kimberlites occur as monogenetic and occasionally polygenetic volcanic entities mostly within ancient cratonic regions of continents. They are commonly preserved as downward tapering pipes and craters which have been infilled with clastogenic mixtures of kimberlite and country rock clasts. Field and Scott Smith (1999) proposed the occurrence of three types of kimberlite bodies, termed Class 1, 2 and 3 by Skinner and Marsh (2004).

Kimberlite bodies of Class 1 can usefully be divided into 3 distinct zones (Hawthorne, 1975): the root zone, the pipe or diatreme facies and the crater facies (Fig. 1). The root zone is made of irregular-shaped bodies of hypabyssal kimberlite and breccias. There are also dykes and sills that occur in association with kimberlite pipes and in some cases dykes can be identified as feeders below and within the root zone. The surface expression of the kimberlite pipe is the crater, which is made up of pyroclastic and re-sedimented volcaniclastic kimberlites. In many cases the crater zone has been removed by erosion (Mitchell, 1986). However, new discoveries in Canada have somewhat changed the paradigm shown in Fig. 1, which is based largely on southern Africa examples. In Canada Cretaceous kimberlites emplaced into Mesozoic host rocks in the Prairies Province are interpreted as bowl and dish-shaped craters filled with volcaniclastic kimberlite without substantial pipes and root zones (Field and Scott Smith, 1999) and have been designated Class 2 kimberlites. Pipes filled with re-sedimented volcaniclastic kimberlite are another variant and have been termed Class 3 kimberlites. We acknowledge that this paper focuses largely on Class 1 kimberlites, because much of the data comes from mature mining operations in southern Africa. Class 2 and 3 kimberlites have only recently been recognised and information on them is largely based on bore-holes and geophysical surveys.

So far no conclusive examples have been found of kimberlite pyroclastic deposits from beyond the crater rim. Also no kimberlite lavas have been authenticated;

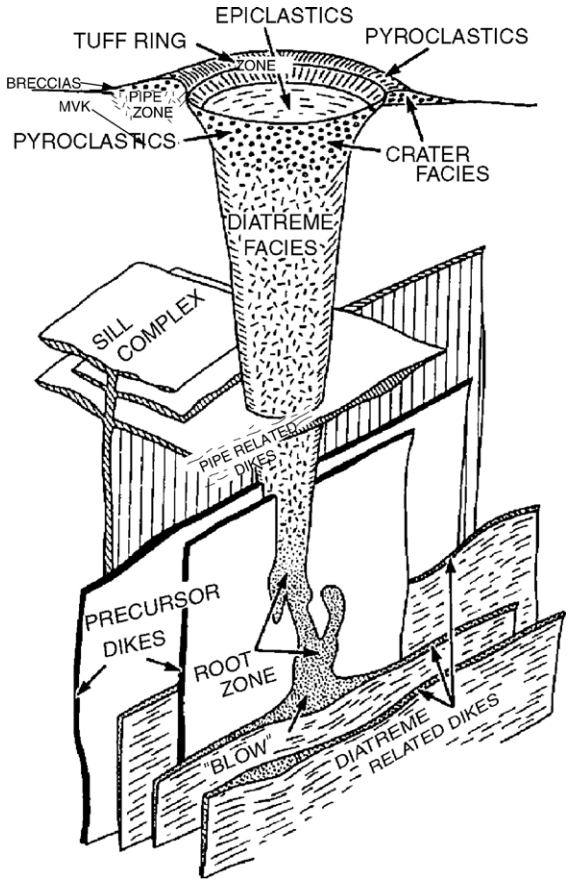

Fig. 1. Illustration showing the characteristic form of a kimberlite pipe from a depth of 2–3 km to the surface. Kimberlite pipes are made up of the root zone, pipe zone and crater zone. Modified after Hawthorne (1975) and Mitchell (1986).

olivine–calcite lavas at Igwisi Hills, Tanzania, however, are similar in many petrological characteristics to kimberlites (Reid et al., 1975). No substantial kimberlite intrusions have been identified that might represent magma chambers. The geological record is biased. Most well-documented occurrences are economic deposits and diamond-rich kimberlites may not be wholly representative.

The ages of known kimberlites vary from early Proterozoic to early Tertiary. Kimberlites have been discovered in all the continents and the current total exceeds 5000 (Kjarsgaard, 1996). Kimberlite pipes and associated hypabyssal intrusions commonly occur in localised clusters of similar age. Clusters may cover areas of several hundreds to thousands of square kilometers. In some examples the clusters are linear in directions parallel to geophysical anomalies in the mantle lithosphere (e.g. Snyder and Lockhart, 2005). Within a cluster sub-groups of kimberlite bodies can be aligned and related to basement structures (Kurszlaukis and Barnett, 2003). Kaminsky et al. (1995) have proposed that structural domes developed in association with kimberlite pipes and fields.

The horizontal dimensions of kimberlite pipes and craters range from a few tens of metres to several hundred metres and they commonly extend to depths from 0.5 to as much as 3 km. Their cross-sectional planform is commonly near circular to ellipsoidal, although less regular and polygonal shapes occur, which seem to be influenced by structures in the country rock. Within clusters two or more kimberlite pipes can overlap with the individual pipes becoming separated at depth where they narrow (Field et al., 1997). The slopes of pipe margins are commonly in the range 60° to nearly vertical with cross-sectional area decreasing with depth. Hawthorne (1975) states that the slope is commonly around 82°. The crater zone is typically flared with gentler inward-dipping slopes than the pipe below (e.g. Field et al., 1997). The shape and dimensions of the root zone are typically more complex and irregular than the pipe; it is quite common for the cross-sectional area to increase with depth in the transition between the pipe zone and the root zone (Clement, 1982). Blind bodies of kimberlite are common with no direct connection to the surface, although they commonly have lateral connections to the main kimberlite pipe. From these typical dimensions cross-sectional areas are commonly in the range 10^3 to 3×10^5 m^2 and volumes of fill in the range 10^6 to over 2×10^8 m^3. These volumes represent minimum magma volumes for the eruptions since the upper parts of pipes have been removed by erosion and poorly constrained volumes of ejecta must have been deposited beyond the crater rim as surface pyroclastic deposits.

2.2. Rock types

Kimberlite pipes and craters are infilled by a variety of volcaniclastic rocks and are commonly associated with subsidiary hypabyssal rocks. Kimberlite rock nomenclature is complex and confused. Some of the problems in nomenclature arise out of premature development of rock names and descriptors, which have been given genetic significance. These names and textural terms are then applied to rocks where the origin is not necessarily well-established. Here we identify four basic types of fragmental rock, while recognising that there are more varieties than these basic types and that some rock types will not fit into this simplified classification. However, the four basic types are widespread and the vast majority of rocks can be so

classified; the classification thus provides a useful starting point. We use the term volcaniclastic since it is not always clear whether clastogenic rocks have a pyroclastic or epiclastic origin.

Here we discriminate two types of volcaniclastic rock: a massive facies and a layered facies. Kimberlite volcaniclastic rocks are made of: juvenile components including lapilli, phenocrysts (dominated by olivine) and groundmass minerals; minerals, thought to be xenocrysts related to break-up of mantle nodules or basement crystalline rocks; a megacryst suite including olivine, ilmenite and garnet; xenoliths of deep origin (such as peridotite and ecologite); and country rock accidental lithic clasts which can be correlated with the geology of the basement and host country rock; and minerals of secondary origin (Clement, 1975; Mitchell, 1986; Skinner, 1989). The kimberlite minerals are commonly dominated by olivine phenocrysts, macrocrysts and xenocrysts. In the majority of cases olivine is replaced by serpentine and other alteration minerals. The groundmass (fine-grained) minerals of kimberlites include variable proportions of spinel, perovskite, olivine microphenocrysts, calcite, serpentine, phlogopite, monticellite, apatite and melilite, although these are not necessarily all found together. Two common varieties of kimberlite are *Group 1*, which are typified by abundant olivine and groundmass perovskite, spinel and monticellite or calcite and *Group 2* where phlogopite becomes a major constituent (Mitchell, 1986; Skinner, 1989; Mitchell, 1997).

In addition to unequivocal igneous minerals the matrices of volcaniclastic kimberlites commonly contain various combinations of diopside microlites, phlogopite microlites, serpentine group minerals, iron oxides (such as magnetite and hematite), sulphides, talc, calcite and clay minerals (such as saponite and smectite). These minerals may relate to vapour phase crystallization from magmatic gases, hydrothermal metamorphism and weathering. Phenocrysts, macrocrysts and xenocrysts of olivine are, in the majority of cases, completely replaced by serpentine and other minerals such as carbonates, talc, oxides and smectite clays. In many cases several episodes of replacement and alteration have occurred. The origin of these matrices and replacement minerals is not so self-evidently igneous and we will return to this topic later. Common components of volcaniclastic kimberlites are "pelletal" lapilli and crystals (also called autoliths) in which primary crystals and accidental lithic clasts are enveloped by a thin rim made up of kimberlite groundmass minerals (Fig. 2a). Such pelletal grains are typically spherical or ellipsoidal. The rims range in thickness from fractions of a millimetre to several centimetres. Juvenile lapilli (Fig. 2b and c) consist of clasts of macrocrysts and phenocrysts set in a kimberlite groundmass. Juvenile lapilli can be quite vesicular (Fig.

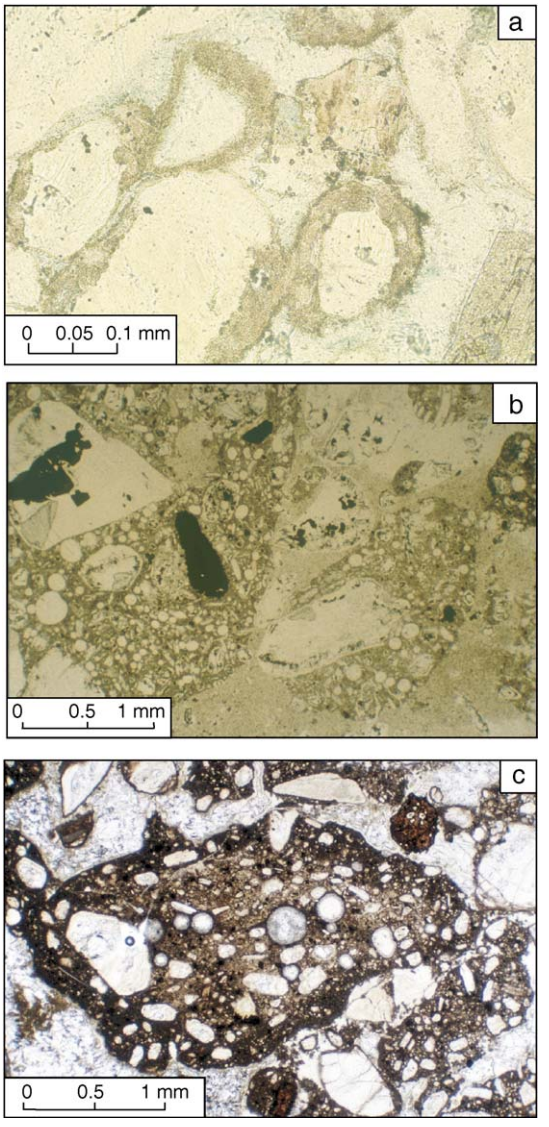

Fig. 2. Photomicrographs of common juvenile components of volcaniclastic kimberlites. (a) Thin rims of kimberlite groundmass around olivine crystals from K1 kimberlite, Venetia, South Africa; the voids between the pelletal crystals are filled with secondary serpentine and diopside microlites, many of which have nucleated on the surfaces of the pelletal crystals. The rims are moulded to one another where they are in contact, suggesting the rims were sticky and deformable with contacts that pinch inwards. (b) Vesicular lapilli in a Fort a la Corne kimberlite, Canada consist of olivine crystals surrounded by kimberlite groundmass with laths of igneous carbonate; abundant clear vesicles are seen. (c) Amoeboid lapilli in a Fort a la Corne kimberlite with plastic margins; the lapilli shows olivine crystals and sparse vesicles.

2b), but amoeboid lapilli shapes with low vesicularities are common (Fig. 2c). Such lapilli are an important component of many Class 2 kimberlites infilling craters and can be recognised in some Class 1 and 3 kimberlites.

Massive volcaniclastic kimberlite is the commonest rock type infilling pipes. Its origin has engendered controversy and it is widely called Tuffisitic Kimberlite Breccia or TKB. This nomenclature is unfortunate for several reasons. First the majority of such rocks contain very few blocks above 6.4 cm so they are not breccias within the conventional classification schemes of pyroclastic rocks (Fisher, 1961; Fisher and Schmincke, 1984; Cas and Wright, 1987). The components of these rocks that are unequivocally primary clasts or grains are typically lapilli to crystals (coarse ash grade: 2 to 1/16 mm) and so they should be described as lapillistone or lapilli tuffs. Second it is unclear whether these rocks contain much fine ash (<1/16 mm). The interstitial matrix in between undisputed lapilli clasts and crystals might be alteration products of fine ash, but alternatively could be secondary minerals filling the original pores of the primary deposit. This latter explanation is consistent with textural evidence for crystal growth into voids, such as euhedral diopside microlites that have nucleated on the surfaces of primary grains enclosing the interstices (Fig. 3). In addition such interstices between grains lack kimberlite groundmass minerals, such as perovskite and spinel, that are resistant to alteration and should be preserved when ash is altered. Third the use of tuffisitic has genetic connotations. Cloos (1941) originally proposed the term tuffisite for intrusive tuffs based on his study of the volcanic necks of Swabia. Since then tuffisite has been used to describe intrusive bodies (e.g. Tuffen et al., 2003). An intrusive origin for the deposits infilling kimberlite pipes may or may not be correct, but highlights the perils of giving rocks names based on processes, especially if the processes are not well understood or controversial. For these reasons we use massive volcaniclastic kimberlite (MVK) as a non-genetic term.

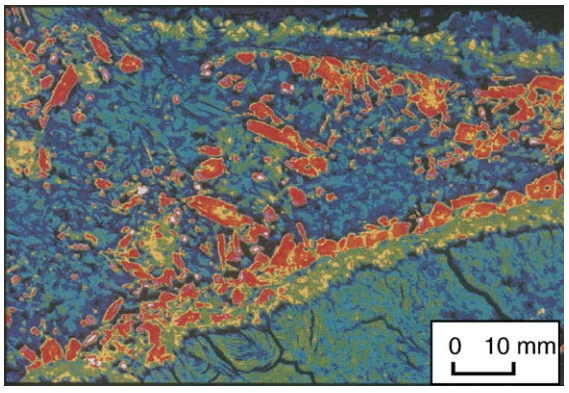

Fig. 3. Photomicrograph of interstitial regions of massive volcaniclastic kimberlite. Skeletal diopside microlites have nucleated on the margins of olivine crystals and grown into the interstices between primary grains. The texture is characteristic of crystals growing freely into void space. The diopside crystals are interpreted as forming as vapour phase crystallization products under high temperature but subsolidus conditions. The remaining void is then filled with secondary serpentine (image from R.H. Mitchell, 1997).

Typical images of MVK are shown in Fig. 4. Country rock lithic clasts are commonly polymict and commonly lithic clasts originate from both shallower and deeper stratigraphic units than the level in the pipe. In MVK the components (crystals, lithic clasts from different sources and juvenile lapilli) have been thoroughly mixed together and variations in proportions of constituents are commonly not easily discernible in the field.

The second rock type of volcaniclastic kimberlite is distinguished by layering and is termed here layered volcaniclastic kimberlite (LVK). There are many subfacies in this category reflecting the wide variety of scales and kinds of layering (Fig. 5). Layering can be picked out by layers rich in lithic blocks and by fluctuations in grain size and sorting (Fig. 5). Layering ranges from diffuse and gradational to well-developed bedding with abrupt internal contacts and internal grading within beds. LVK tends to be best developed in those kimberlites like Orapa (Botswana) where the shallow crater facies is preserved, but layered kimberlites can be found in the deep parts of narrow pipes, particularly towards the margins. There are many examples of LVK where the beds dip into the pipe or crater centre at angles of order 30–40°, consistent with an origin as avalanches, talus or grain flows dipping into the pipe centre at the angle of repose; well-documented examples include Orapa, Botswana (Field et al., 1997); Venetia, South Africa (Kurszlaukis and Barnett, 2003), Koffiefontein, South Africa (Naidoo et al., 2004) and Mwadui, South Africa (Stiefenhofer and Farrow, 2004). Experimental studies by Riedel et al. (2003) show that the angle of repose is higher when granular material is dipping into the centre of a narrow container; for many materials the repose angle increases from around 30° to almost 40°. Some varieties of LVK, particularly those in shallow crater-fill environments, can be ascribed to primary pyroclastic processes (e.g. tephra fall, pyroclastic flows and surges) and others are epiclastic related to redistribution of primary deposits by reworking. Terms such as pyroclastic kimberlite (PK) or resedimented kimberlite (RVK) or epiclastic kimberlite (EK) might then be appropriate if the origin is not in

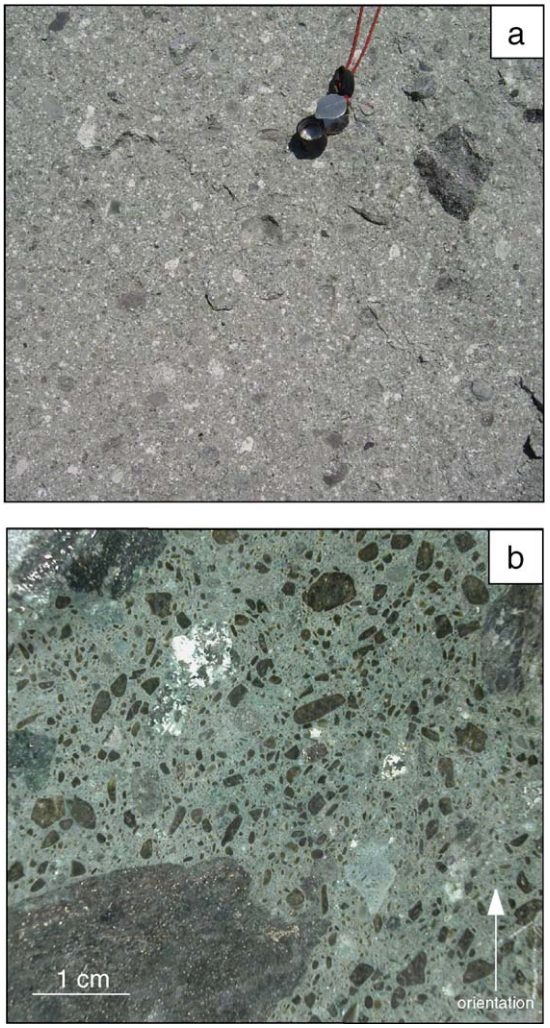

Fig. 4. Typical outcrops of massive volcaniclastic kimberlite. (a) MVK at Orapa mine, Botswana shows the typical massive appearance with olivine crystals and lithic clasts prominent. The dark angular lithic clasts include Karoo basalt clasts and Karoo sedimentary rocks derived from higher stratigraphic levels at 180 m or more above the level of exposure. The white clasts are granite basement clasts derived from at least 300 m below the exposure level. Note that there are no blocks above 6.4 cm diameter in the image. Hand lens is 1 cm diameter. (b) Slab of MVK (K1 unit) at Venetia mine showing lithic clasts, dark rounded olivine megacrysts in a matrix of small serpentinised olivine crystals and void-filling minerals (dominantly diopside and serpentine). The orientation arrow shows the vertical direction and a near vertical fabric of elongate olivine crystals is discernible.

doubt (nomenclature after Field and Scott Smith, 1998). However, the origin is commonly not clear.

Marginal wall-rock breccias are the third prominent rock type. They range from breccias entirely composed of wall rock to breccias with variable amounts of kimberlite matrix of the MVK variety; these latter breccias vary from net-veining of in situ brecciated wall rock (Fig. 6a) to clast-supported breccias to matrix-supported varieties (Fig. 6b and c). Some breccias are monomict and can be divided into those that correspond to the adjacent in situ wall-rock lithology and those that juxtapose a different (typically stratigraphically higher) lithology against the in situ wall rock (Fig. 6). Others are polymict and mix together rocks from different stratigraphic levels. Breccias characterised by distinctive lithic assemblages can commonly be mapped in the field and underground to delineate distinctive stratigraphic units (e.g. Field et al., 1997; Kurszlaukis and Barnett, 2003; Naidoo et al., 2004; Stiefenhofer and Farrow, 2004). Breccias that bring stratigraphically higher wall rocks to deeper levels have been described as subsidence breccias (Barnett, 2004). Some breccias show structures and textures similar to those encountered in volcanic debris avalanches (Glicken, 1998; Clavero et al., 2002; Voight et al., 2002) where coherent and commonly large domains of fractured and brecciated rock types are mixed together incompletely to form a heterogeneous breccia. Some domains of a single rock type are broken into elongate trains similar to the more highly sheared facies of debris avalanches (Francis et al., 1985; Glicken, 1998; Voight et al., 2002). Examples are also found where marginal breccias are intruded as neptunian dykes into the wall rock.

Crude layering is observed in some breccias; angles are commonly in the 30° to 40° range consistent with an avalanche origin, but examples of steeper dip angles are known. In some cases the layering is a cryptic fabric and in others is a well-defined alternation of breccia and MVK or LVK. In most cases the layering dips into the centre of the pipe at angles consistent with typical angles of repose, suggesting debris sliding into the interior. Layered facies are more prominent in shallow levels and

Fig. 5. Well-bedded volcaniclastic kimberlite (LVK) defined by the alternation of coarse and fine layers of lithic clasts. Locality is in the middle of the Jwaneng Central Pipe, Botswana.

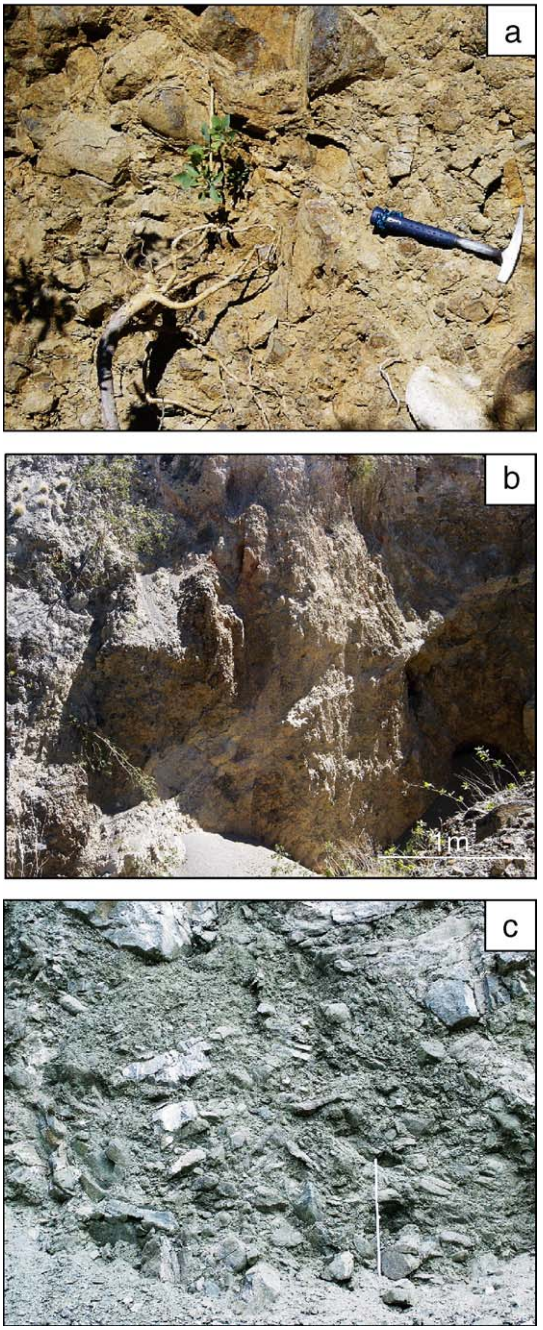

Fig. 6. Examples of marginal breccias. (a) A dolerite wall-rock breccia at the margin of the Wimbledon kimberlite located at the Record Stone Quarry in the Kimberley district, South Africa. The dolerite has been displaced by faults at the margin of the pipe. The dolerite is disrupted but has not been invaded by kimberlite veins. (b) Kimberlitic marginal breccia in the Wimbledon kimberlite showing a breccia of shale and dolerite with kimberlite matrix. (c) Clast-supported volcaniclastic kimberlite breccia in the K2 pipe, Venetia Mine South Africa. The rule in the picture is 1 m in length.

crater facies, but also occur in the deep parts of pipes. As a generality layering becomes more diffuse and disappears into the pipe centre where MVK tends to dominate. Matrix supported massive breccias are gradational into MVK.

The fourth main rock type is magmatic kimberlite (MK), which is found as coherent, lobate, irregular or ellipsoidal bodies (in plan view) within kimberlite pipe fills and is a characteristic facies of the root zones of kimberlites. Such rocks are distinguished here from dykes and sills, which have sharp and planar intrusive contacts. The irregular magmatic facies kimberlite commonly grades into undoubted fragmental MVK and LVK through rocks with transitional characteristics. These rocks typically contain lithic clasts, which are commonly strongly altered due to reactions with kimberlite magma. Magmatic kimberlites are termed hypabyssal kimberlites by many kimberlite geologists. They are described (Skinner and Marsh, 2004; Hetman et al., 2004) as uniformly textured, coherent rocks with abundant macrocrysts and a groundmass containing typical kimberlitic minerals (e.g. monticellite, spinel, perovskite, calcite and serpentine). Transitional rocks that are gradational between MVK and MK show globular structures in which the fine-grained rims of several pelletal lapilli appear fused together at their contacts (Fig. 2a). Areas between the globular structures are filled with late stage minerals, such as diopside, phlogopite, apatite, serpentine and calcite.

The origin of MK and its relationship to the transitional rocks and MVK are open questions. According to Skinner and Marsh (2004) they originate as hypabyssal intrusions of kimberlite, which then segregate volatiles in situ to form MVK by catastrophic degassing with the transitional rock types, preserving the early stages of volatile exsolution. However there are alternative interpretations. One possibility is that such bodies are intrusive into plastic deposits (i.e. MVK prior to lithification), as happens in subglacial volcanics where irregular lobes, pods and distorted sheets intrude into hyaloclastite piles (e.g., Tuffen et al., 2001). However, such intrusive bodies generally maintain abrupt contacts with clastic host rocks. An alternative interpretation is that MK rocks have a clastogenic origin in which rapid accumulation of hot pyroclastic material leads to agglutination, welding (sintering), lithification by vapour phase crystallization and partial to complete elimination of pore space. Such processes are widespread in all common magma types forming agglutinates, welded tuffs, vapour phase zones in ignimbrites, rheomorphic tuffs and clastogenic lava (Smith, 1960; Fisher and Schmincke, 1984; Cas and Wright, 1987;

Sumner, 1998). Such clastogenic rocks also occur as high-level intrusions and vent fills (e.g. Reedman et al., 1987; Sparks, 1988). Re-constitution of pyroclastic materials into dense lava-like rock tends to become more extreme in low viscosity magmas (e.g. Schmincke, 1974; Sumner, 1998), with original pyroclastic textures being sometimes completely obliterated and only gradational contacts with undoubted pyroclastic rocks and preservation of entrained lithic clasts providing evidence of a clastogenic origin. The abundance of microlitic diopside and phlogopite in some transitional rocks can be compared to vapour phase zones of ignimbrites that commonly are transitional between densely welded and non-welded zones (Smith, 1960).

We favour the welding hypothesis as an alternative to the volatile segregation and explosive hypothesis. Welding, vapour phase lithification and clastogenic origin of lava-like rocks are well-established processes, whereas we know of no example of the direct in situ preservation of volatile exsolution and explosive magma fragmentation processes. Highly dynamic processes (e.g. Alidibirov and Dingwell, 1996; Sparks, 2003) are by their nature very hard to preserve. Dykes and sills commonly intrude MVK, but they have sharp rather than gradational contacts and the typical tabular geometry of unequivocal hypabyssal intrusions. A key observation is that the contacts of pelletal lapilli pinch inwards (see Fig. 2a), consistent with the disequilibrium contacts expected by sintering of hot grains. If the spaces between the lapilli were due to gas exsolution (segregation) from melt rounded contacts formed due to surface tension forces would be expected.

2.3. Geometric relationships of kimberlite facies

The geometrical arrangement of different facies and rock units in kimberlite pipes takes a variety of forms. In geological maps rock units commonly exhibit a concentric outcrop pattern around the margins of the pipe (Clement, 1982; Field et al., 1997; Kurszlaukis and Barnett, 2003; Ekkerd et al., 2003; Stiefenhofer and Farrow, 2004; Skinner and Marsh, 2004; Naidoo et al., 2004; Webb et al., 2004), as exemplified by the Finsch kimberlite in South Africa, the Koffiefontein pipe in South Africa, the Mwadui pipe in Tanzania and the Orapa kimberlite in Botswana (Fig. 7). Marginal breccias commonly separate the pipe wall from MVK in the centre of the pipe with both gradational and abrupt contacts. Commonly such breccias only occur on some margins with other margins having a direct contact of MVK with wall rock. Some abrupt contacts appear to be faults and in some cases two, three or more distinct breccia lithologies have steeply dipping contacts against one another. In some pipes, such as Letlhakane, Botswana and Finsch, South Africa (unpublished company data), several different MVK units have been identified from different lithic contents or mineralogy or diamond grade. These units are also typically arranged concentrically with respect to the pipe margins with very steep internal contacts with one another (Figs. 6 and 7), which can be abrupt or gradational. The dips of contacts are invariably towards the pipe centre and are typically 50° to vertical, much higher than the repose angles of granular materials (Fig. 7b). Although concentric patterns are common they are not necessarily symmetric (Fig. 7).

2.4. Secondary alteration

The majority of volcaniclastic kimberlites have been pervasively altered, with serpentine being the most important alteration mineral. In most volcaniclastic kimberlites olivine is pseudomorphed by serpentine (Mitchell, 1986). Textures are typically complex with more than one episode of replacement. Other typical minor alteration minerals replacing olivine in different examples include carbonate, talc, magnetite and brucite. Lithic clasts are also variably altered with the mineral assemblages depending on the lithology. In addition to serpentine and carbonate chlorites are common; in altered dolerite clasts for example. Serpentine veins are common. Serpentinisation reactions are not isochemical and large amounts of water are required (Evans, 1977, 2004; Palandri and Reed, 2004). The reactions consume oxygen and thus the associated fluids are strongly reduced and are highly alkaline. Large volume changes of up to 50% are involved when olivine is replaced. The original shapes of euhedral olivine phenocrysts are commonly preserved in pseudomorphs and so large amounts of Mg and lesser amounts Si must be transported into the fluid phase. Serpentinisation reactions take place predominantly at moderate to low temperatures (Hyndman and Peacock, 2003; Palandri and Reed, 2004; Evans, 2004) with about 600 °C being the upper limit for antigorite and about 400 °C for lizardite (Evans, 2004). The simplest explanation of serpentinisation in volcaniclastic kimberlite is that it is a consequence of post-emplacement and sub-solidus hydrothermal metamorphism.

The origin of matrix serpentine in volcaniclastic kimberlites is important with regard to inferring the original nature of the deposits. In MVK from Class 1 kimberlites very small diopside microlites have void-filling textures (Fig. 3) in the interstices between

primary crystals, lapilli and lithic clasts. The remainder of the interstices is typically filled with later serpentine. The textures (Figs. 2a and 3a) are similar to packstone textures in calcarenite and oolitic limestones where calcite is the cement and to textures in sedimentary concretions where, for example, sulphide replaces original cements. In many examples of VK (e.g., Orapa, Venetia, Letlhakane, Kimberley and Premier) the interstices are mostly free of the groundmass minerals of kimberlite that are more resistant to alteration (e.g., spinel and perovskite). Interstitial serpentine is sometimes attributed to replacement of glass or the product of late-stage magmatic fluids (Skinner and Clement, 1979; Clement and Reid, 1989). In the volcaniclastic kimberlites this origin is hard to reconcile with the common absence of exotic late stage kimberlitic groundmass minerals in the interstices and the void-filling textures. We infer that the interstices represent original pore space, which was infilled by precipitation from hydrothermal fluids: similar conclusions were reached by Clement (1979) and Mitchell (1986). The source of the serpentine is the Mg and Si removed into the fluid phase during alteration of olivines, xenocrysts and diverse lithic rock types. We suggest that volcaniclastic kimberlites were initially formed as deposits with high porosities (10–30%) and high permeabilities. In particular MVK and LVK rocks were formed as sand and gravel grade deposits and did not contain much fine ash; if this ash had been generated in the eruption then it must have been removed by eruptive processes.

The origin of the common matrix assemblage diopside and serpentine can be constrained by consideration of mineral equilibria in the $CaO–MgO–SiO_2–H_2O–CO_2$ system (Fig. 8) using the calculation methods in Connolly (1990) and Holland and Powell (1998). At 50 MPa the assemblage antigorite–diopside–dolomite is confined to temperatures below 520 °C and is only stable at low mole fractions of CO_2 less than about 0.10. One source of serpentinising fluid is water-rich kimberlite magma. The 10% to 15% water required for serpentinisation cannot be dissolved in silicate melts except under mantle pressure conditions, but water is highly soluble in carbonate melts even at low pressure (Keppler, 2003). Thus kimberlite magmas with carbonatite affinities might therefore be able to degas sufficient water to cause extensive serpentisation. The requirement of low CO_2 content in the fluid, however, is inconsistent with the fluid being derived from a CO_2-rich magma. Rather the mineral assemblage and stable isotope data (Sheppard and Dawson, 1975) are consistent with external water circulating through the host kimberlite pipe-fill after emplacement. To our knowledge tremolite has not been widely described from kimberlites, yet would be expected as a common phase if the partial pressures of CO_2 were high. These results are consistent with the findings of Hyndman and Peacock (2003), who found that brucite, a common alteration mineral in kimberlites, coexists with serpentine at temperatures below 500 °C.

3. Physical constraints on kimberlite eruptions

In this section we consider various aspects of kimberlite eruptions from a dynamical viewpoint. Over the last three decades much has been learnt about the dynamics of volcanic eruptions with the development of mechanical models of magma transport, magma flows and explosive flows within conduits and out into the atmosphere. Many of the principles established from these studies should apply to kimberlites, albeit taking account of the differences in properties between kimberlite magmas and more common magma types, such as inferred very low viscosity and very high volatile contents. Combination of the constraints provided by geological observations and constraints based on the physics of eruptions provides the basis for developing a model of kimberlite volcanism.

3.1. The nature of kimberlite magmas

There is considerable uncertainty about the compositions of kimberlite magmas. Key physical properties that govern eruptive processes, such as viscosity, temperature, volatile content and volatile solubility, are not well constrained. Inferences about magma compositions come from studies of the geochemistry and petrology of the rocks, but such studies are made difficult due to physical contamination by lithic clasts, xenoliths, xenocrysts and macrocrysts, and by the pervasive effects of hydrothermal metamorphism and alteration. Olivine is the dominant mineral phase and typically occurs as large crystals (0.1 to several mm). Commonly the olivines are inferred to be a mixture of phenocrysts precipitated from the kimberlite magma, xenocrysts formed by disruption of mantle nodules and olivines that are part of a megacryst suite precipitated with minerals like garnet and ilmenite from kimberlite and kimberlite-like magmas at very high pressure (Mitchell, 1986; Skinner, 1989; Mitchell, 1997; Le Roux et al., 2003). The high abundance of olivine crystals in both volcaniclastic and hypabyssal kimberlites indicates that many erupt as porphyritic magmas, but aphanitic varieties are found (Price et al., 2000; Le Roux et al., 2003; Harris et al., 2004). The groundmass mineralogy

in Group 1 kimberlites includes variable combinations of microphenocrystal olivine, carbonate (calcite or dolomite), serpentine, monticellite, spinel, apatite, perovskite, melilite and ilmenite (Mitchell, 1986). Group 2 kimberlites have abundant phenocrystal and groundmass phlogopite.

Several methods have been used to estimate the original composition of kimberlite magma. The groundmasses of hypabyssal intrusions have an aphanitic texture (Edgar et al., 1988), and have been considered true melt compositions (Watson, 1967; Dawson, 1973). Rims of groundmass minerals around

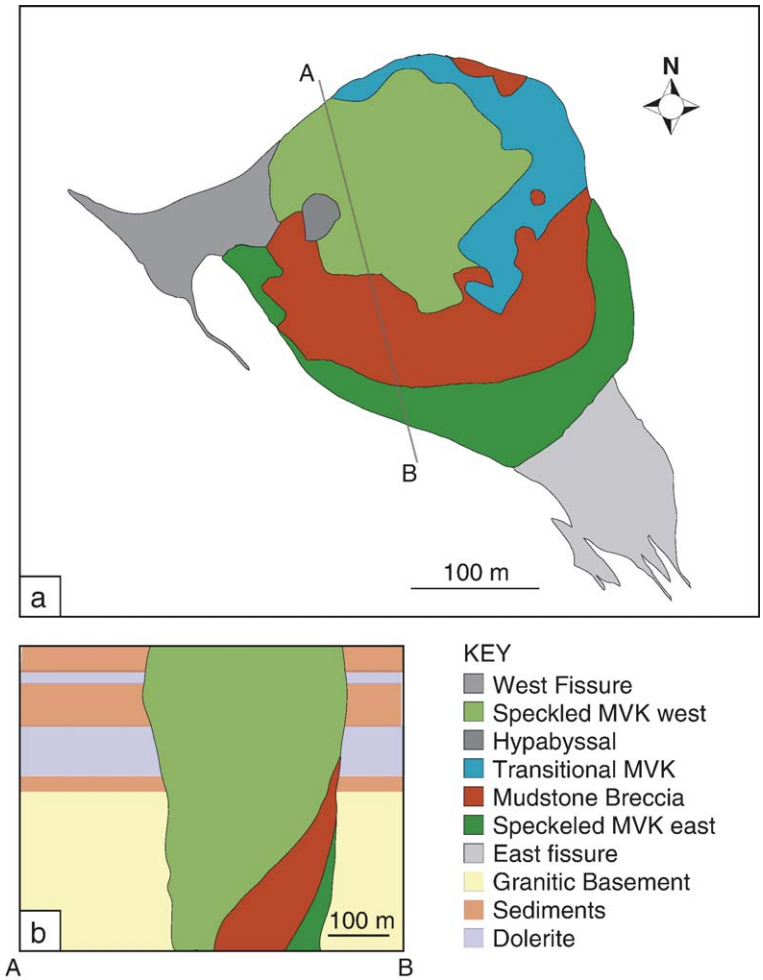

Fig. 7. (a) Geological map of Koffiefontein kimberlite pipe, South Africa showing the concentric arrangement of lithofacies (after Naidoo et al., 2004). The concentric arrangements of kimberlite and wall-rock derived breccias are noteworthy. (b) Cross-section through the Koffiefontein pipe showing that the internal contacts between the concentrically zoned units dip into the pipe interior at angles well above the angle of repose. (c) Oblique 3D Geological model of the Finsch kimberlite pipe, South Africa (after Ekkerd et al., 2003). The red and yellow zones are breccias composed of abundant lithic clasts of Karoo (Stormberg) basalt (red) and mudstone (yellow). F1 and F8 kimberlite types are volcaniclastic kimberlite, whilst the F2 and F4 are a magmatic plug and late-stage dykes, respectively. The F3 and F5/6 kimberlites are pre-cursors that have both magmatic and volcaniclastic components. The N–S and E–W dimensions of the 3D box are approximately 410×450 m, respectively. There is no vertical exaggeration. (d) Surface plan view of the Finsch kimberlite. Annotation as above in (c). (e) Oblique 3D model of the Mwadui kimberlite pipe, Tanzania, after Stiefenhofer and Farrow (2004). Here the concentric arrangement of peripheral breccias shown in red and purple are noteworthy, as is the geometry of the re-sedimented facies shown in green, brown and yellow. The pipe at surface is approximately 1.5×1.2 km in size. The numbered dots are the locations of drill holes used in the study by Stiefenhofer and Farrow (2004). (f) 3D Geological model of the Orapa A/K1 kimberlite, Botswana. The pink, purple and brown units are all breccias derived from country rock lithologies. The brown breccias are basalt-dominated, the purple sandstone-dominated and the pink, lower Karoo shale and Basement dominated. All the other lithologies are volcaniclastic kimberlites with varying proportions of country-rock clasts. The maximum east–west and north–south dimensions are approximately 950×1600 m, respectively. The vertical extent of the model is from the current (un-mined) surface to a depth of 660 m below surface.

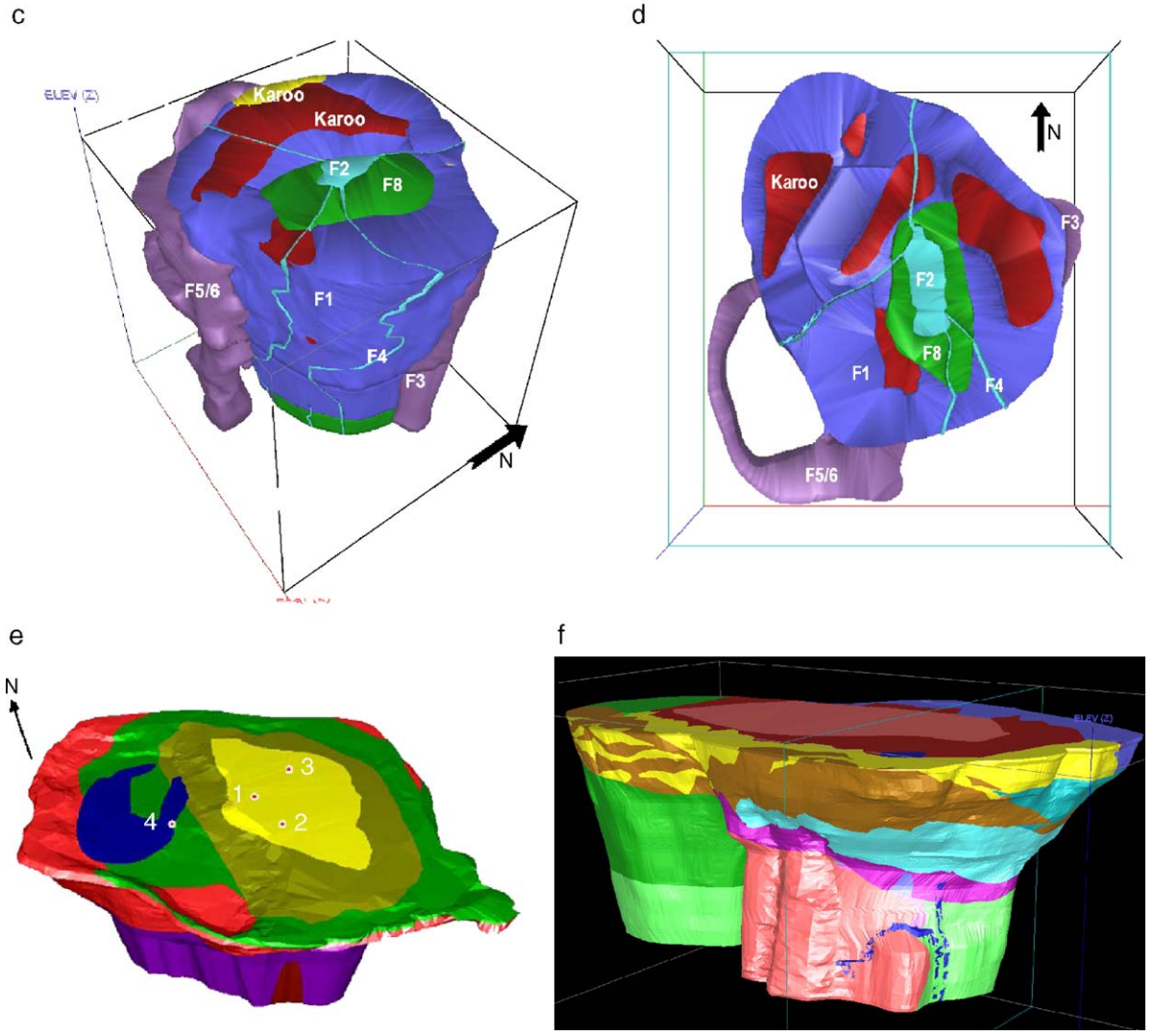

Fig. 7. (*continued*)

pelletal lapilli and quite rare fine-grained hypabyssal rocks have provided estimates of melt compositions. Ferguson et al. (1975) proposed that the compositions of fine-grained groundmasses around nucleated autholiths represented melts (column 1, Table 1). Price et al. (2000) studied the aphanitic margins of kimberlite from the Jericho Pipe, Northwest Territories, Canada, on the Slave Craton (column 2, Table 1). Le Roux et al. (2003) studied the bulk compositions of kimberlites from the Kimberley area and identified rocks using geochemical and petrological criteria, which had been affected by crustal contamination or break-up of garnet lherzolite nodules. For the remaining rocks, which were mostly aphanitic samples collected from the margins of hypabyssal intrusions, Le Roux et al. (2003) found variations that they interpreted as the consequence of fractional crystallization of an olivine–calcite assemblage. Using criteria such as Mg Number, Ni contents and trends on variation diagrams they estimated a primary magma composition (column 3, Table 1). Harris et al. (2004) studied three aphanitic and several macrocrystic samples from the Uintjiesburg kimberlite, South Africa (column 4, Table 1). They estimated the primary magma composition on the basis of the intersections of the geochemical trends of the major rock types; aphanitic rocks were interpreted as defining an olivine–phlogopite fractionation trend and macrocrystic rocks as defining a mixing trend of primary melt with macrocrysts. Golovin et al. (2003) studied secondary melt inclusions in olivine from unaltered

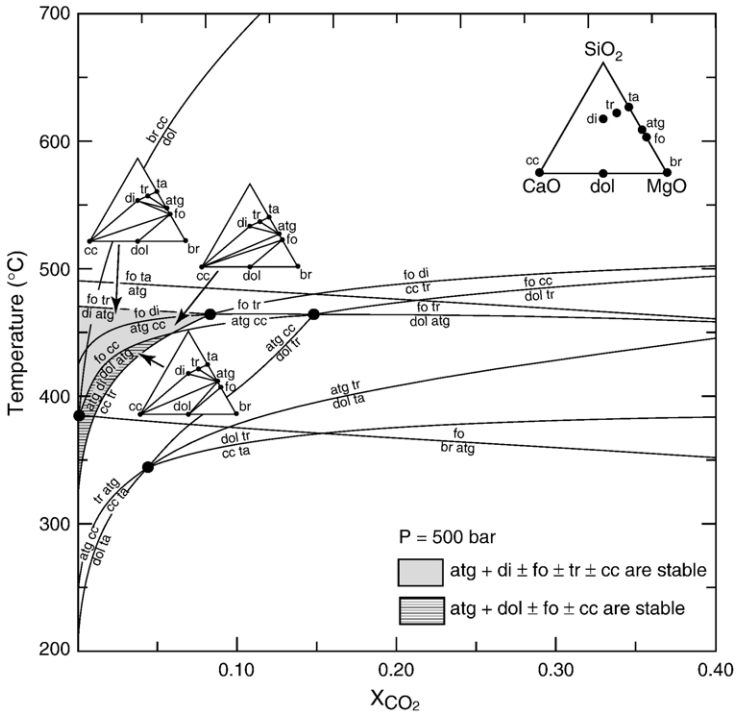

Fig. 8. Phase equilibria in the SiO_2–MgO–CaO–CO_2–H_2O system at 50 MPa showing the stability fields of the common matrix minerals in volcaniclastic kimberlites and major metamorphic reactions. Ta: talc; fo: fosterite; dol: dolomite; atg: antigorite; tr: tremolite; di: diopside; br: brucite. The fields where the common matrix-fill mineral assemblage antigorite (serpentine)–diopside–dolomite and antigorite–diopside are stable are shown.

kimberlite and estimated the melt composition shown in columns 5 (Table 1). Taken together the available estimates indicate that kimberlites are dominantly composed of SiO_2, MgO, FeO and CaO with subsidiary constituents of Al_2O_3, TiO_2 and K_2O (Table 1). In comparison to other magma types kimberlite magmas are silica poor (25–30%) and strongly silica undersaturated.

Consideration of melt generation processes combined with the explosive character of kimberlite eruptions have led to a consensus that kimberlites are volatile-rich magmas with CO_2 and H_2O being the main volatile constituents (Eggler, 1978; Wyllie, 1980). However, it is not straightforward to estimate volatile contents. Aphanitic samples from pipes and hypabyssal intrusions, such as those studied by Price et al. (2000), are mainly composed of serpentine and calcite with other minerals being minor. These minerals are also described from the rocks studied by Le Roux et al. (2003) and Harris et al. (2004). However, the volatile contents of the rocks (Table 1) are unlikely to be simply related to the volatile contents of the magmas. Serpentine may largely originate as a secondary alteration product due to interaction with external non-magmatic water, formed at temperatures below 500 °C (Evans, 1977; Fig. 8), and it is not easy to distinguish primary igneous carbonate from the products due to hydrothermal metamorphism (see Fig. 8) and low temperature alteration. Examples of primary igneous carbonate (calcite or dolomite), however, have been recognised from diagnostic textures and distinctive minor element concentrations (e.g., high Sr or Mn contents) in some hypabyssal rocks (Dawson and Hawthorne, 1973; Mitchell, 1984; Armstrong et al., 2004), in the groundmasses of some juvenile lapilli (Mitchell, 1997) and in the Uintjiesberg kimberlite (Harris et al., 2004). Even when primary igneous carbonate is recognized whole rock data do not necessarily reflect the CO_2 content of the magma since the CO_2 is in fact governed by the stoichiometry of the carbonate minerals. Such occurrences indicate a close association of kimberlites with carbonatite magmas (Bailey, 1980). A plausible interpretation of groundmass monticellite is that it is the consequence of degassing of CO_2 from a CO_2-rich ultramafic melt in which CO_2 is largely present as CO_3 in association with CaO. When the CO_2 exsolves monticellite becomes the stable silicate phase.

Table 1
Some estimates of kimberlite melt compositions

Values in wt.%	1.	2.	3.	4.	5.
SiO_2	33.60	35.66	32.73	29.56	34.35
TiO_2	3.76	0.76	1.82	3.82	1.79
Al_2O_3	3.34	1.83	2.67	2.74	2.82
FeO	14.05	7.97	10.90	11.24	9.80
MnO	0.31	0.19		0.22	0.18
MgO	24.80	29.35	32.73	30.80	36.88
CaO	16.14	22.46	14.55	17.73	12.45
Na_2O	0.29	0.37		0.07	0.35
K_2O	1.96	0.54	2.42	1.35	0.92
P_2O_5	1.48	0.87	2.18	2.21	0.46
Cr_2O_3	0.27			0.26	
CO_2	7.00	13.02	7.00	8.63	6.9
H_2O^+	7.44	6.68	8.00	4.92	

The compositions have been normalised to 100% free of the volatile constituents (H_2O and CO_2) to facilitate comparison. The volatile estimates reported by the different studies are also listed. 1. Average composition of fine-grained groundmass around autoliths in Lesotho kimberlites (after Ferguson et al., 1975); 2. Average of 6 compositions of kimberlite collected from the aphanitic margins of the Jericho Pipe, Canada (after Price et al., 2000); 3. Indicative melt composition deduced from compositions of aphanitic intrusions, Kimberley by Le Roux et al. (2003) noting that the composition has been slightly modified from the published estimate following a personal communication from A. Le Roux; 4. Primary melt composition estimated by Harris et al. (2004) for the Uintjiesberg kimberlite, South Africa; 5. Estimate of kimberlite melt composition based on study of secondary melt inclusions (Golovin et al., 2003).

Phlogopite is a common primary mineral and indicates that the magmas must have contained water. There is no direct way of estimating how much water might be present, but high water contents would help to explain the lack of strong contact metamorphic effects and fluidity of kimberlite dykes and sills. Kimberlite magmas crystallize olivine and commonly evolve towards a carbonatitic water-rich residual melt. Water is very soluble in carbonatite melts and also reduces the liquidus of such melts by hundreds of degrees (Wyllie and Tuttle, 1960; Keppler, 2003); at only 1 kbar the saturated water content might be as much as 10 wt.% and liquidus less than 700 °C. Exsolution of water from very water-rich melts near the Earth's surface may be the main cause of the highly explosive character of kimberlite eruptions.

Estimates of temperatures in the source regions of kimberlites are in the range 1200 to 1400 °C based on studies of mantle nodules (see Priestley et al., in press). These temperatures are about 400 °C below the dry solidus of peridotite and so the presence of volatiles or volatile-bearing phases are required in the source region to enable melt production. Dalton and Presnall (1998a) show, for example, that carbonated peridotite has solidus temperatures in the 1200 to 1400 °C range and that carbonatite and kimberlite melts can be generated by small degrees of partial melting.

Models for the generation of kimberlite melts remain controversial. One widely held view is that kimberlites are generated by partial melting at the base of the mantle lithosphere in the thick cool and metasomatised roots of Archean continents, as suggested by studies of macrocrysts and geochemical arguments (e.g. Gurney et al., 1993; Tainton and McKenzie, 1994). Conditions for melt generation were suggested by Bailey (1980), who proposed that kimberlites form when the solidus of carbonated mantle is in grazing incidence with the geotherm at 150–200 km depth. Bailey (1984) also proposed that the mantle must have been metasomatised by volatiles to form a heterogeneous source, characterised by a stockwork of veins. Tainton and McKenzie (1994) estimated the source compositions of kimberlites as ancient depleted mantle metasomatised by melts enriched in exotic and volatile components. Experimental studies demonstrate that melt compositions similar to kimberlitic rocks can be generated at small degrees of partial melting of carbonated peridotite (Wyllie, 1980; Dalton and Presnall, 1998a,b). Such melts vary from almost pure carbonatites to silicate melts containing large amounts of dissolved CO_2 (5% to 20%). On this basis kimberlites are inferred to be rich in CO_2 and sometimes water. The melt compositions generated in experiments on synthetic analogues of carbonated peridotite are similar to those estimated from studies of natural rocks. For example, the primary kimberlite composition estimated for Kimberley (Table 1, Column 3) is similar to compositions formed by 0.6% to 0.7% partial melting of carbonated lherzolite (Dalton and Presnall, 1998a) with 7 wt.% CO_2.

Other researchers have argued that kimberlites must be formed deep in the asthenosphere and in association with mantle plumes (e.g. Ringwood et al., 1992; Haggerty, 1994), influenced by the discovery of majorite in diamond inclusions (Moore and Gurney, 1985; Tappert et al., 2005). Ringwood et al. (1992) inferred that kimberlites originate in the transition zone of the mantle (400 to 650 km depth), based on experimental studies which establish under what conditions majorite is in equilibrium with kimberlite melts. Haggerty (1994) links kimberlites ultimately with volatile release from the core associated with deep mantle plumes. Tainton and McKenzie (1994) consider that the discovery of majorite only constrains the origin of some diamonds to the transition zone and not the kimberlite melts. They also point out that Group 2

kimberlites have evolved isotopic compositions that are consistent with the source being part of the continental lithosphere.

Magmatic processes at low pressures equivalent to the crust or eruptive conditions are poorly constrained in comparison to information on high-pressure conditions. Le Roux et al. (2003) found systematic relationships between Ni and Mg number in aphanitic kimberlites at Kimberley that he explained by fractionation of olivine and calcite in the ratio 70 : 30. Calcium zoning profiles in olivines from mantle xenoliths in the Gibeon Kimberlite, Namibia suggest that olivines resided in the upper mantle for weeks in their host kimberlite before being erupted (Franz et al., 1996). Unfortunately there are no data or phase equilibria of composition similar to those in Table 1 under low-pressure conditions relevant to eruptions (0–2 kbars). Temperatures for melt generation are fairly well constrained at high pressure (1200–1400 °C), but are poorly constrained at low pressure. An unresolved issue is how to explain the apparently high CO_2 contents of kimberlite magmas. Studies in the system SiO_2–MgO–CaO–CO_2 at moderately high pressures of 2 GPa by Moore and Wood (1998) and at 2.7 GPa by Lee et al. (2000) indicate that melts with SiO_2 of 25 to 30% and high CO_2 contents in equilibrium with mantle assemblages can only exist over a very narrow temperature range. Outside this range either the melts are carbonatite at lower temperatures or silicate melts (45 to 50% SiO_2) with moderate amounts of dissolved CO_2 at higher temperatures. In the later case solubility measurements (Brooker et al., 2001) indicate that silicate melts would degas most of the CO_2 at the low pressures within pipes and associated hypabyssal intrusions. Most kimberlite groundmass minerals (e.g. monticellite, phlogopite, perovskite) suggest that the residual melts are silicate melts, but residual groundmasses dominated by unequivocal igneous carbonate also occur.

Apart from these experimental studies there are other clues as to the nature of kimberlite magmas. Pelletal lapilli and olivine crystals commonly have a very thin coating of groundmass minerals (Fig. 2a) interpreted as quench melt and are commonly very rounded, suggesting that surface tension has governed their shape. Kimberlite hypabyssal intrusions are typically thin (<1 m) and can sometimes form subsidiary vein-systems with veins only a few centimetres thick. These two observations suggest viscosities much less than high temperatures primitive basalts. Hypabyssal rocks and juvenile lapilli only occasionally have amygdales; the scarcity of vesicles is consistent with very low viscosity melts from which gas bubbles segregate very easily when the magma stagnates.

Viscosities of kimberlite melts can be constrained from recent experimental studies of peridotite melts (Dingwell et al., 2004) and aqueous fluids at high pressure (Audetat and Keppler, 2004). The peridotite melt studied by Dingwell et al. (2004) has viscosities in the range 0.7 Pa s at 1500 °C to 1.5 Pa s at 1200 °C. This melt is somewhat more silica-rich than typical postulated kimberlite compositions so the viscosity is anticipated to be lower than these values on the basis of the melts being less polymerised than peridotite melts. Addition of dissolved water may reduce viscosity further. However, the reduction of viscosity with increasing water contents observed in more polymerised melt compositions (Audetat and Keppler, 2004) may not be as pronounced in melts which are not strongly polymerised. On the basis of the available experimental evidence viscosities are estimated to be in the range 0.1–1 Pa s. Large proportions of entrained xenocrysts and olivine phenocrysts will increase viscosity substantially; crystal-laden kimberlite melt could have viscosities of order 10 to 100 time greater than the melt (Pinkerton and Stevenson, 1992). Degassing and rapid cooling under near surface or eruptive conditions can lead to rapid groundmass crystallization, either increasing viscosity or causing abrupt solidification.

In summary available observations, together with inferences from geochemical and experimental studies, indicate that kimberlites are magmas, predominantly made of SiO_2, MgO and CaO, have very low viscosity and are magmas with high volatile contents (principally CO_2 and probably water).

3.2. Magma ascent in dykes and supply rates

A first order control on volcanic processes is the supply rate of magma. In the case of kimberlites the geological evidence, geophysical data and physical intuition indicate supply through vertical fractures (dykes). Kimberlite dykes are typically in the order 0.3 to 1 m in width and 0.5 to 10 km in breadth (the horizontal length) (Mitchell, 1986). The observed breadths of kimberlite dykes are surprisingly short given that the magma ascends from depths of order 200 km. Snyder and Lockhart (2005) document seismic shear wave anisotropy in the lithosphere of NW Canada, closely associated with linear kimberlite pipe clusters. They interpret these data as kimberlite dyke swarms in the lithosphere. The lengths of the anomalous zones are up to 50 km, indicating that feeder dykes may have longer breadths at depth and decrease on approaching

the Earth's surface; a result consistent with analogue experimental results (Menand and Tait, 2002). Dyke dimensions are comparable to those observed in many basaltic eruptions. These typical dimensions can be used to place constraints on magma flow conditions. Magma propagation in dykes and flow through dykes once they have reached the surface are now quite well understood from development of fluid dynamic and mechanical models (e.g. Wilson and Head, 1981; Huppert and Sparks, 1985a,b; Rubin, 1995; Lister and Kerr, 1991; Menand and Tait, 2002). The propagation rate of dykes is principally governed by the ability of magma to flow into the fracture tip (Lister and Kerr, 1991; Rubin, 1995).

An overpressure P_e is required to open a dyke of width $2w$ over a length b by the following relationship (Lister and Kerr, 1991):

$$w = 2bP_e(1-v^2)/E \quad (1)$$

where v is Poisson's ratio and E is the elastic modulus. If, for example, $P_e \sim 10$ MPa (a typical tensile strength of crustal rocks), b is of order 1 km, $v=0.25$ and $E=37.5$ GPa then $2w=1$ m. This width is comparable to those observed in kimberlite and basalt dykes, taking into account that the width of flowing dykes may be about twice as much as the final solidified width (Menand and Tait, 2002). Thus the dimensions of the dykes are consistent with driving pressures comparable to the tensile strength of crustal rocks and to the pressure conditions encountered in basaltic eruptions.

Related issues are whether the dykes are likely to be connected to the deep source and why their breadths are so short. If h (the dyke vertical length) were, for example, 200 km with $b=1$ km then, for $2w=1$ m, the volume in the dyke would be 2×10^8 m^3, comparable to the volume of the larger kimberlite pipes. A vertical dimension that is much greater than the horizontal breadth is certainly required as the volume in a dyke 1 km × 1 km × 1 m is much smaller than most pipes. Experiments by Menand and Tait (2002) show that dykes maintain a near constant breadth when buoyancy is the cause of overpressure. However, their experimental study concerned a system with homogeneous stress distribution. The crust typically has a deviatoric stress system with dykes propagating normal to σ_3. Lateral propagation can be prevented if the maximum horizontal stress (σ_2 or σ_1) is larger than the pressure in the dyke. Typical crust is strongest at the base of the upper crust with values of deviatoric stress being of order 10 to 15 MPa. The observation that the breadths of kimberlite dykes are not particularly long indicates that overpressures have not greatly exceeded these strength limits and the constraints of the stress field. Buoyancy overpressure is given by:

$$\Delta P = \Delta\rho g h \quad (2)$$

where ΔP is the overpressure, $\Delta\rho$ is the density difference between the magma in the dyke and the crust or lithosphere averaged over the vertical length, g is gravitational acceleration and h is the vertical length of the dyke. If, for example, $g \sim 10$ m s^{-2}, $h=10$ km and $\Delta\rho=100$ kg/m^3 then $\Delta P=10$ MPa. Thus only modest buoyancy is required to obtain reasonable overpressures in the crust. Despite the high content of dense olivine a low density for volatile-rich kimberlite magma can be easily achieved.

Two alternative models have been proposed for dyke propagation. Most studies favour the propagation rate being determined by a balance between buoyancy or source overpressure and the frictional pressure drop (Lister and Kerr, 1991). Menand and Tait (2002), however, have shown that fluid-filled cracks can propagate under steady state conditions, where the buoyancy is balanced by the fracture pressure, P_f, given by:

$$P_f = K/(\pi h)^{1/2} \quad (3)$$

where K is the stress intensity at the fracture tip. Field estimates of K are in the range 10^2 to 10^3 MPa m$^{1/2}$ (Reches and Fink, 1988; Scholtz et al., 1993; Atkinson, 1994). If for example $K=500$ MPa m$^{1/2}$ and $h=10$ km then $P_f=10$ MPa. Propagating fluid-filled fractures have a tadpole shape with a head that is significantly wider than the following tail. However, as recognised by Menand and Tait (2002), the two alternative models are similar in that, at steady state, the head of the dyke is fed by a much longer tail; this would be the case with kimberlites if the tail is connected to the source at 200 km. Thus the balance between frictional resistance and driving pressure in the tail governs the supply rate. Menand and Tait (2002) propose that steady state is achieved when the buoyancy balances the fracture pressure at a critical length h_c:

$$h_c = P_f/\Delta\rho g \quad (4)$$

For $\Delta\rho=100$ kg/m^3 and $P_f=10$ MPa, $h_c=10$ km. The model of Menand and Tait (2002) may be favoured for kimberlite because of the suspected very low viscosity of the magma. We therefore need to analyse the role viscous resistance could play in kimberlite dyke propagation, in particular in the tail region.

The flow regime in the dyke depends on the Reynolds number defined as:

$$Re = 2w\rho u/\mu \quad (5)$$

where u is the velocity, ρ is the magma density and μ is the viscosity. If Re is low (<10 then viscous forces dominate and the flow is in the laminar regime. If Re is high (>10^3) then inertia dominates the flow, viscosity is negligible and the flow is in the turbulent regime. A critical value of the viscosity between these regimes can be estimated if the dyke width is known and a critical dyke width can be estimated if the velocity is known by equating the viscous pressure with the overpressure resulting in:

$$\mu_c = [(2\Delta P\rho w^3)/(3hRe_c)]^{1/2}; \quad (6a)$$

$$w_c = [(3\mu^2 hRe_c)/(\Delta P\rho)]^{1/3} \quad (6b)$$

where Re_c is a chosen threshold between laminar and turbulent flow. Turbulent flow is expected when $\mu<\mu_c$ and $w>w_c$. By choosing an upper limit on h (~200 km) the viscosity threshold can be reduced to a minimum value and the dyke width threshold maximised. For ΔP=10 MPa, w=0.5 and ρ=3000 kg/m^3, the viscosity threshold is 12.4 Pa s for Re_c=10 and 1.24 Pa s for Re_c=10^3. The viscosity threshold at Re_c=10 is at least one order of magnitude greater than the inferred viscosities of kimberlite magmas. The viscosity threshold for fully turbulent conditions (Re_c=10^3) is at the high end of the estimates of kimberlite melt viscosities. Thus we conclude that kimberlite magmas are transported in the turbulent regime.

Note that in this case elastic constraints are satisfied for Eq. (6a) provided b=1000 m (see Eq. (1)).

For the thickness threshold the relationship between width and pressure has also to be satisfied. By combining Eqs. (1) and (6b) we obtain:

$$w_c = [6b\mu hRe_c(1-v^2)/\rho E]^{1/4} \quad (7)$$

Choosing the same representative values of parameters and a representative viscosity of 0.3 Pa s we obtain w_c=0.32 and 0.09 m for Re_c=10^3 and Re_c=10, respectively. Provided dykes are wider than these threshold values turbulent flow is again inferred.

Having established that high Reynolds number conditions are likely we can apply the analysis of Lister and Kerr (1991) for the propagation of a fluid filled crack under turbulent conditions with wall fraction. Assuming that the buoyancy is the main driving pressure their analysis gives the velocity as:

$$u = 7.7[w^5/\{\mu(\rho g\Delta\rho)^3\}]^{1/7} g\Delta\rho \quad (8)$$

where the factor 7.7 has been determined experimentally. Note the very weak dependence of velocity on the magma viscosity making it unimportant that we lack detailed knowledge of kimberlite magma viscosity. Taking a range of dykes width $2w$=0.1 to 0.5 m, a viscosity of μ=0.3 Pa s and representative density contrasts of 100 and 300 kg/m^3 we obtain velocities from 2.9 to 16.8 m/s (Table 2). In all cases the Reynolds numbers are of order 10^3 or greater. A lower limit on velocity arises because dykes that are too thin or too slow will freeze. This can be approximately estimated by calculating a distance, L_T, (known as the thermal entry length) following Lister and Kerr (1991):

$$L_T = uw^2/\kappa \quad (9)$$

where κ is the thermal diffusivity ($\kappa=5\times10^{-7}$ m^2/s). By choosing L_T=200 km we calculate a minimum dyke width of $2w$=0.32 m for $\Delta\rho$=100 kg/m^3 and 0.24 m for $\Delta\rho$=300 kg/m^3. These results in turn imply minimum velocities for kimberlite ascent speeds of about 4 m/s. Velocities in these ranges are consistent with ascent times estimated from studies of garnet dissolution (e.g. Canil and Fedortchouk, 1999) and data on Ar isotope profiles in phlogopites (Kelley and Wartho, 2000). They are also consistent with transport of dense xenoliths. In a low viscosity fluid the settling velocity, V_s, of a xenolith of diameter, d, gives a lower bound on velocity:

$$V_s = C_d(\Delta\alpha gd/\alpha)^{1/2} \quad (10)$$

where C_d is the drag coefficient (of order unity), α is the magma density and $\Delta\alpha$ is the density contrast. Taking for example $\Delta\alpha$=500 kg/m^3 and d=0.5 m then the ascent speed must be greater than 1 m/s. The size of transported xenoliths may in fact be constrained by the dyke width rather than velocity. Finally we note that these calculations do not take account of the exsolution and expansion of gas, which will be considered further below.

3.3. Volumetric flow rates and eruption durations

These estimates of ascent speed (>4 to 16 m/s) can be combined with observations of dyke widths (0.3 to 1 m)

Table 2
Calculations of ascent speeds of dyke-transported kimberlite magma using Eq. (8) in text

Dyke width ($2w$) (m)	Velocity $\Delta\rho$=100 kg/m^3	Velocity $\Delta\rho$=300 kg/m^3
0.2	2.9	5.4
0.3	3.8	7.2
0.6	6.3	11.7
1.0	9.1	16.8

and lengths (0.5 to 10 km) in kimberlite feeder zones to indicate magma supply rates in the range 500 to 10^5 m^3/s. Estimates of minimum kimberlite eruption volumes in the range 10^6 to 2×10^8 m^3 suggest durations of several hours to several weeks. However these durations are likely to be shorter than actual durations for two main reasons. First the volume estimates are lower bounds because they do not include the amount of magma ejected to the surface away from the crater rim. Below we develop in the discussion section arguments to suggest that the volume trapped in the pipe is only a small fraction of the total erupted magma. Second the driving pressure in the source region may decline as an eruption proceeds (as is common in basaltic eruptions) leading to an exponential decrease of magma supply rate (Stasiuk et al., 1993). In these circumstances time averaged supply rates will tend towards the lower estimates of magma supply rate. These estimates of duration and flow rate overlap with durations of typical continental monogenetic volcanic eruptions, but the inferred flow rate range extends to higher values more typical of Sub-plinian and Plinian explosive eruptions. The range of flow rates from 500 to 10^5 m^3/s would generate eruption columns in the range 10 to 35 km (Sparks et al., 1997); thus many kimberlite eruptions may be Plinian in intensity and style which implies that much of the ejecta reaches into the stratosphere.

3.4. Volatile behaviour during kimberlite magma ascent

The case for a magmatic origin of the explosive eruption of kimberlites is based on the volatile-rich nature of the magma, in particular CO_2. Here we present some preliminary calculations on the degassing of kimberlite magma to place some constraints on eruptive conditions. An initial temperature of 1400 °C is assumed based on available experimental investigations (Ringwood et al., 1992; Dalton and Presnall, 1998a,b) and data on xenoliths derived from the presumed source region (Boyd and Nixon, 1975).

Exsolution and expansion of volatiles during magma ascent are expected to be a major influence on kimberlite eruptive processes. We assume that CO_2 is the volatile species and comment below on what differences might arise if water were a significant component. We chose a linear solubility law:

$$x = sP \tag{11}$$

where x is the weight fraction of dissolved CO_2, s is the solubility coefficient and P is the pressure (in Pascals). The solubility of CO_2 increases as melts become more silica undersaturated (Blank and Brooker, 1994; Brey and Ryabchikov, 1994; Brooker et al., 2001) and we have used $s=3\times10^{-9}$ Pa^{-1}. This value has the convenient property that the model melt is just CO_2 saturated for $CO_2=20$ wt.% at 200 km depth and is also consistent with available experimental data (Brooker et al., 2001). An unresolved issue is the extent to which kimberlite melts might evolve from or alternatively evolve towards carbonatite melts. In such melts CO_2 solubility may not be pressure dependent and the dissolved melt composition can have very high proportions of CO_2 even at low pressure governed by the stoichiometry of the carbonate melt and Eq. (2) would not apply. If residual melts evolve towards carbonatite melt residual during ascent then it is feasible to imagine that melts never become CO_2 saturated because the solubility increases too fast. Some group 1 kimberlites, however, have largely silicate groundmasses, so the assumption of solubilities for silicate melt systems seems reasonable. However, there are examples of carbonatite groundmasses rich in primary igneous calcite (Mitchell, 1997) as well as carbonate-rich sills (e.g. Dawson and Hawthorne, 1973). In this case the explosivity might arise either because water is an important volatile or because there is a low-pressure decarbonation reaction. The lack of low pressure experimental data on kimberlite melts is a barrier to making progress on these matters.

The thermodynamics is treated as follows. We assume a melt adiabat of 0.3 °C/km of ascent. We relate the density of exsolved CO_2, ρ_{CO_2}, to pressure from the NIST database by a power law:

$$\rho_{CO_2} = 0.012P^{0.56} \tag{12}$$

Although at high pressure CO_2 does not behave ideally (Spera, 1984) most of the gas exsolution, expansion and cooling takes place at low pressure where the ideal behaviour is reasonable.

Fig. 9 shows the volumetric fraction of exsolved gas as a function of pressure expressed as a depth equivalent assuming lithostatic pressure conditions. The conversion between pressure and depth assumes a density of 2600 kg/m^3. We note that the approximation that the pressure and depth can be equated will not be correct close to the Earth's surface where conduit flows can become under-pressured or overpressured, but is a sufficiently good approximation to indicate the depths at which vesiculation becomes significant. The depth equivalent at which the magma reaches 70% vesicularity is also shown. For the gas contents inferred to be typical of kimberlite the magma becomes very vesicular at crustal depths. For example at a pressure equivalent of about 30 km a magma with 10 wt.% CO_2 has a

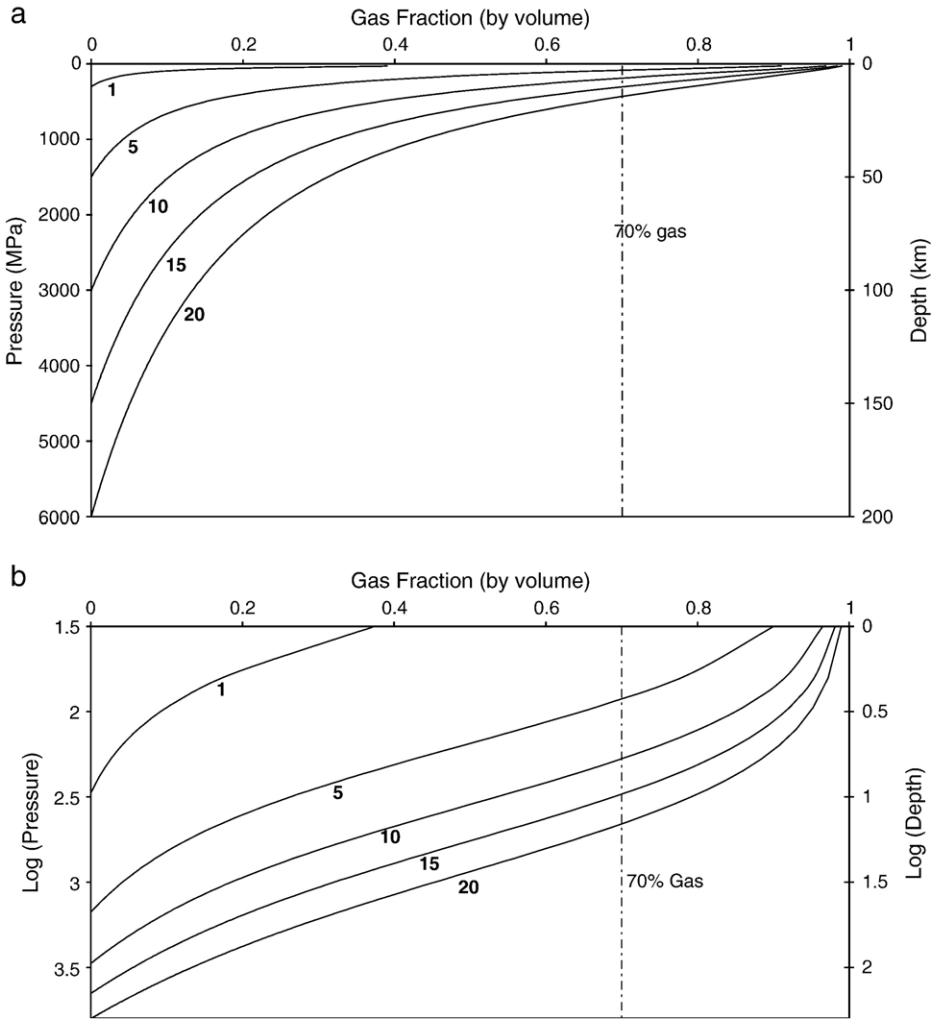

Fig. 9. (a) Volume fraction of gas as a function of depth for different CO_2 contents. In the diagram the pressure is shown on the left hand vertical axis and the depth equivalent (assuming a lithostatic pressure gradient) is shown on the right hand vertical axis. In the calculations the zero depth pressure is one atmosphere. The vertical dashed line references 70% volume percentage of bubbles and is the vesicularity at which fragmentation is expected. (b) The same calculations as (a) but on a log scale and showing the shallow level relationships in more detail. Depth unit is km and pressure unit is MPa.

vesicularity of 30%, which is high enough for bubble coalescence to become a significant factor. If 70% is used as an approximate threshold for fragmentation then this condition can develop at pressures with depth equivalents of several kilometres. Below we consider in more detail how such very gas and bubble-rich magmas might behave in the final several kilometres of ascent.

Gas exsolution and bubble expansion accelerate the magma to speeds in excess of the calculations shown in Table 2. For example 75% vesiculation will accelerate the magma 4 times the velocity of the unvesiculated magma for the same conduit cross-sectional area.

3.5. Temperature variations

High-pressure experiments, consideration of geotherms, and mantle xenolith studies suggest that temperatures in the deep source are in the 1200 to 1400 °C range (Priestley et al., in press). Canil and Fedortchouk (1999) note that garnet xenocrysts should dissolve in only a few minutes at the source temperatures and infer that eruption temperatures of 1000–1200 °C are consistent with the preservation of garnet. Phillips and Harris (2003) studied co-existing mineral inclusions in diamonds to deduce average crystallization temperatures and pressures. They estimated temperatures of 1270 °C at 6.1 GPa for non-touching inclusions

and 1070 °C at 5.3 GPa for touching inclusions. Magmas cool during ascent and eruption. Abundant crystallization of olivine phenocrysts in many kimberlites suggests either cooling or strong degassing. Cooling mechanisms during magma ascent include adiabatic expansion of gas-rich magma, heat transfer to the walls of the transporting dyke (Huppert and Sparks, 1985b), endothermic reactions with mantle minerals, and entrainment of xenoliths during ascent.

Fig. 10 shows the temperature of the magma as a function of depth based on only the thermodynamics of gas exsolution; this baseline model ignores all other thermodynamic and fluid dynamic effects. The temperature at a depth of 5 km (assuming lithostatic pressure conditions) is also shown in the inset table. To a first approximation the surface cooling is about 32 °C for each 1 wt.% CO_2 with a CO_2 content of 20 wt.% causing the magma to cool to below 900 °C. Most of the cooling occurs in the final stage of ascent; for example at a pressure equivalent to a depth of 10 km the model with 10 wt.% CO_2 is at 1270 °C whereas the final temperature at one atmosphere is 1040 °C. These results confirm that adiabatic gas expansion is going to be a significant factor in cooling magma containing significant volatiles. Similar results would be obtained if water were used as an alternative or in addition to CO_2, except that the shallow cooling would be even more pronounced due to the expected higher solubility of water as a function of pressure.

Heat transfer to the walls of the dyke can result in significant cooling. Huppert and Sparks (1985b) have calculated temperature decreases of 100 to 300 °C for the turbulent ascent of komatiite magmas in dykes through the lithosphere. Entrainment of mantle xenoliths can cause additional cooling. However, these cooling processes are counteracted by olivine crystallization. The latent heat for olivine is assumed here to be 250 kJ kg^{-1}, based on experimental measurements by Stebbins and Carmichael (1984) and Stebbins et al. (1983). Taking the specific heat of the melt as 1200 J kg^{-1} K^{-1} 50% olivine crystallization can raise the temperature by over 100 °C. In principle a thermodynamical and fluid dynamical model of kimberlite magma ascent could be developed that integrates these various effects together. However, any model results will be highly uncertain because of the large uncertainties associated with the volatile contents and lack of data on the phase equilibria of kimberlite magmas under the low pressure conditions pertinent to eruptive conditions.

Cooling in the eruptive environment may be large due to mixing with shallow level lithic clasts within the pipe and mixing with external water during eruption and mixing with cold air during explosive processes within the pipe and above the crater. Low emplacement temperatures for volcaniclastic kimberlite have been inferred from the lack of metamorphic effects on entrained xenoliths (Watson, 1967; Skinner and Marsh, 2004). Sosman (1938) deduced a temperature of 380 °C from a study of the thermal effects on coal inclusions. Stasiuk et al. (1999) interpreted reflectance values in dispersed organic matter to deduce emplacement temperatures in the range 150 to 650 °C for volcaniclastic kimberlites.

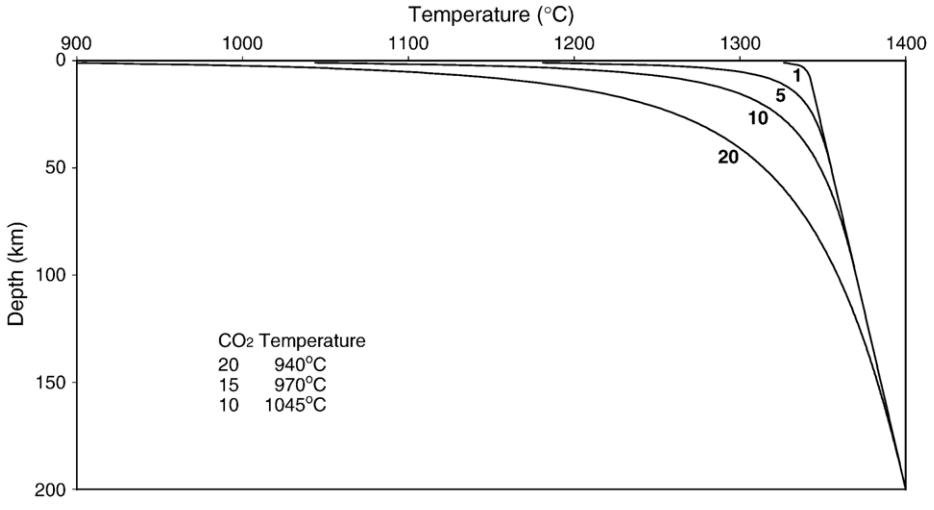

Fig. 10. Temperature as a function of depth for different CO_2 contents. The inset table gives exact calculated values of temperature at a pressure equivalent to a depth of 1 km assuming lithostatic conditions.

3.6. Near surface explosive flows

Explosive flows in volcanic conduits are complex (see for example Sparks et al., 1997; Papale, 1999; Melnik and Sparks, 2002). Here we develop some approximate and simplified models. Our purpose is to show that kimberlite eruptions evolve from overpressured to pressure-adjusted vent exit conditions. This pressure evolution has a major influence on the evolution of the pipe and its consequent geology.

Explosive flows in volcanic conduits eruptions are commonly limited by the speed of sound in the erupted mixture, known as choked flow conditions (Woods, 1995). Choking occurs when the cross-sectional area of the vent is smaller than some critical value below which the mixture exits the vent at a pressure above atmospheric (overpressured). As a rough approximation the choked speed, U_c, is given by (Sparks et al., 1997):

$$U_c = 0.95(nRT)^{1/2} \quad (13)$$

where R is the gas constant for the gas, n is the exsolved gas content and T is the temperature in Kelvin. Here we take a representative kimberlite to have a temperature of 1000 °C and exsolved CO_2 and H_2O contents of 10% and 5% so that R=235.2 J kg K^{-1}. This gives a representative speed of 200 m/s. The critical vent radius, r_c, for a given volume flow rate of magma (expressed as dense magma and excluding any bubbles) can be calculated by taking the exit pressure equal to one atmosphere, and the mixture density of the representative kimberlite to be 4.3 kg/m^3. When the vent cross-section is above the critical value then the exit pressure is expected to be close to one atmosphere (i.e. pressure-adjusted).

Fig. 11 shows calculations of the critical radius for the magma flow rate range of 300 to 10^5 m^3/s. The diagram divides up conditions into overpressured and pressure-adjusted regimes. Supply rates as high as 10^5 m^3/s will always be in the pressurised regime for typical radii of kimberlite pipes, but for most supply rates the eruption is expected to start in the overpressured regime when the pipe is narrow and move into the pressure-adjusted regime when the pipe widens sufficiently. Fig. 11 shows schematically two eruption paths with supply rate remaining constant (path 1) and supply rate declining with time as the pipe widens and deepens simultaneously (path 2).

When the exit pressure falls to one atmosphere, the vertical velocity will depend on the flow conditions within the pipe. The slope of the pipe margin, frictional interactions with the wall and entrainment of the atmosphere are some of the factors that control the

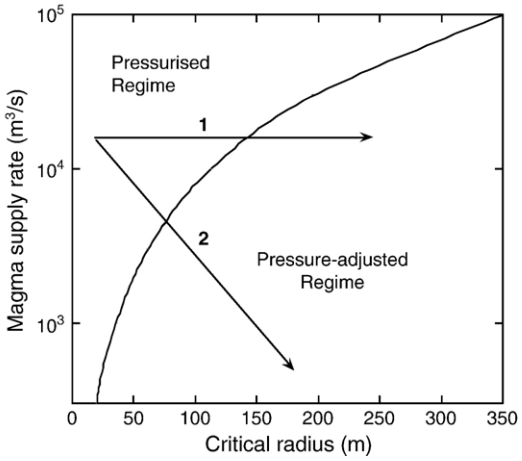

Fig. 11. Calculations of the critical radius at which the exit pressure is exactly one atmosphere for magma flow rates ranging from 300 to 10^5 m^3/s. The curve for this critical condition divides eruptive conditions into an overpressured regime where choked flow conditions arise and a pressure-adjusted regime where the exit conditions are at one atmosphere. In the later regime the flow can become greatly underpressured at depth with respect to the lithostatic pressure in the conduit wall. Two eruption paths are shown with magma supply rate remaining constant (path 1) and magma supply rate declining with time as the pipe widens and deepens simultaneously (path 2).

flow. Pressure-adjusted volcanic flows into the atmosphere spread by entrainment with a spreading rate of about 1 in 8 (Wilson, 1976). This is a slope of 7° measured against the vertical and is comparable to the slope of kimberlite pipes; Skinner and Marsh (2004) suggest a typical value of 8° against the vertical (i.e. a pipe slope of 82°). Thus pipes are sufficiently steep-sided that entrainment will be inhibited and we can assume mass conservation will hold. If the pipe is more flared, as might be expected in the crater, then air entrainment will become important. A useful approximation for a steep-sided pipe then is to calculate the mean vertical velocity as a function of flow rate.

Fig. 12a shows the variations of mean vertical velocity as a function of pipe radius ($r > r_c$) and magma supply rate in the pressure-adjusted regime. The velocity rapidly falls as the pipe radius increases. This result is central to considering the mechanism of filling the pipe with kimberlite ejecta, because the velocity determines the size of particles that can be entrained by the flow out of the pipe. The maximum diameter, d_m, of pyroclast that can be erupted is determined by comparing the terminal fall velocity of the clast in the gas phase with the exit velocity. The terminal velocity, V_t, is given by (Sparks et al., 1997):

$$V_t = C_d[(\Delta\alpha g d_m)/\alpha_g]^{1/2} \quad (14)$$

where C_d is the drag coefficient of order unity, $\Delta\alpha$ is the density contrast between the clast and the gas, and α_g is the gas density. For our representative case the gas density is 0.56 kg/m^3 and we take $\Delta\alpha = 3000$ kg/m^3. The significance of the pressure-adjusted regime becomes clear and the results of the calculations are shown in Fig. 12b. For the choked condition of 200 m/s the threshold clast diameter is about 0.8 m. In the pressurised regime blocks of this size and larger can be ejected with the size being dependent on the exit pressure. Eventually, as the pipe widens and deepens, the flows become too weak to transport particles out of the vent and ejecta coarser than the diameter threshold must become trapped within the pipe. As the pipe widens the size threshold decreases rapidly and can eventually become comparable to the size of, for example, olivine crystals in the 1 cm to 1 mm range. At this stage only fine particles can escape with the gas. We suggest that the pipe then starts to fill up with coarser particles and becomes a fluidised bed as developed in the next section.

3.7. Fluidisation

Fluidisation has been long invoked as a major process in pyroclastic flows (e.g., Sparks, 1976; Wilson, 1984) and in kimberlite volcanism (Dawson, 1971; Woolsey et al., 1975; Clement, 1982; Mitchell, 1986). The concept has been used in rather different ways and so the kimberlite literature is at times unclear. Here we only use fluidisation as a term that describes a bed of particles, which develops fluid-like properties as a consequence of the flow of interstitial gas. We do not use fluidisation to describe the disruption of brittle rocks by high-pressure gases or fluids, although dilatant fractures can be intruded by gas-particle mixtures, which might meet the criteria for being fluidised systems (see Fig. 6c). A bed of particles becomes fluidised when the drag of the gas flow through the bed equals the bed weight.

In the previous section we show that once the pipe has become wide enough to be in the pressure-adjusted regime then favourable conditions for developing a fluidised bed arise. The gas flows become too weak to transport particles out of the pipe and these must either accumulate in the pipe or be reduced in size and elutriated. Fig. 13 shows the variation of fluidisation velocity with grain size calculated using the Ergun equation (see Wilson, 1984) and using CO_2 as the gas at a temperature of 700 °C and for particles of density 3300 kg m^{-3}. For a straight-sided container, there will be a range of particles that can be fluidised at a given gas velocity from the maximum size that can be transported

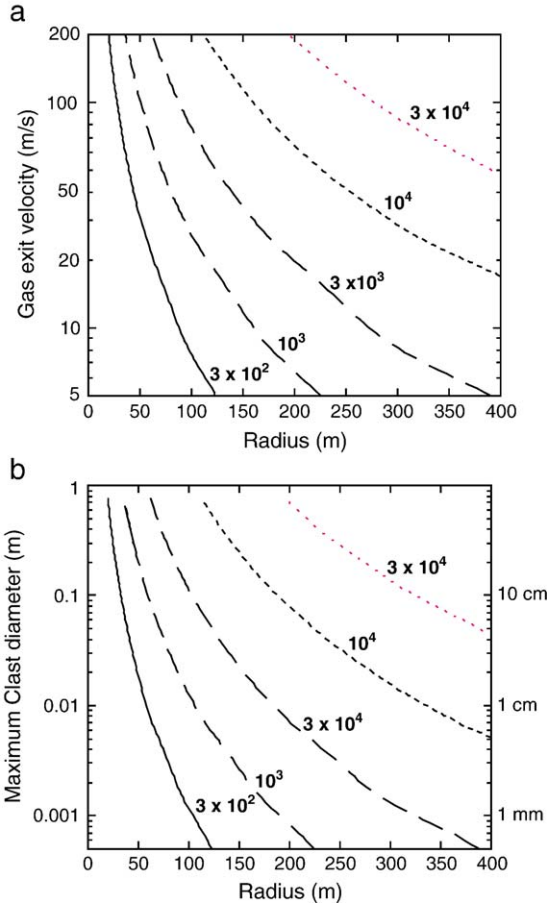

Fig. 12. (a) Variations of mean vertical velocity as a function of pipe radius ($r > r_c$) and magma supply rate in the pressure-adjusted regime. (b) Variations of the particles size (diameter) that can be ejected from the vent using the criterion that the exit velocity of the gas equals the terminal velocity of the particle.

from the vent (the elutriation condition) to the maximum size. Larger particles than this latter maximum are expected to fall through the bed to its base, assuming that they have a larger density than the bed. Particles in the 0.01 to 1 cm size range are dominant in the MVK facies and are consistent with gas velocities in the 1 to 10 m/s range. Thus the origin of the MVK is attributed to the waning phase of the eruptions when the pipe is wide and deep and the supply rates of magma have declined.

A difficulty with the fluidisation hypothesis is that the range of particles in typical MVK (Walters et al., 2006-this volume) is much wider than the range of particle sizes that can be simultaneously fluidised and thoroughly mixed (see Wilson, 1984). Walters et al. (2006-this volume) propose on the basis of experimental observations that the range of particle sizes that can be

simultaneously fluidised and mixed together is larger in a diverging container geometry.

Walters et al. (2006-this volume) present fluidisation experiments that suggest how the concentric arrangement and steep internal contacts can develop between different VK and marginal breccia units within kimberlite pipes. In the experiments gas is passed through a bed of sand with coloured marker bands. The gas flow forms a flared region of fluidised sand bounded by undisturbed sand with the geometry of a pipe (Fig. 14). The material for the marker bands is completely mixed homogeneously within the fluidised interior and this process provides a mechanism for the thorough mixing observed in MVK facies in the interior of kimberlite pipes. The width of the pipe increases and the angle between disturbed and undisturbed sand decreases as the gas velocity increases. The gas flow creates a circulation in the disturbed region with up flow along the centre and down flow along the margins. Surface marker bands can slump down the margins to mimic the geometry of marginal breccias. If the gas supply is turned off and then switched on again at a lower velocity then an internal contact between the new fluidised zone and the earlier fluidised zone forms. The contact is steep at angles well above the angle of rest or internal friction angles of the sand (Fig. 14), mimicking the geometric relationships of internal contacts between VK units in kimberlites. These experiments thus support a model in which the volcaniclastic pipe fills are the consequence of gas fluidisation.

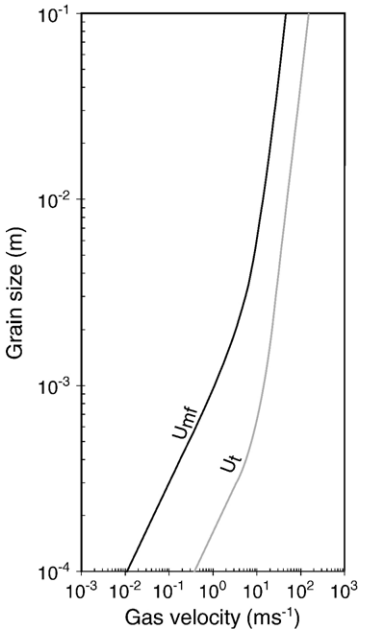

Fig. 13. The variation of the minimum fluidisation velocity (U_{mf}) and terminal velocity (U_t) with grain size for particle beds fluidised by CO_2 at temperatures of 700 °C. The density of the particles is 3300 kg m^{-3} and assumed voidage is 0.45. For a given vertical gas velocity particles in a range size that can meet the criterion $U_t > U > U_{mf}$ can be stable within the fluidised bed. Particle for which $U > U_t$ will be elutriated from the bed and those for which $U < U_{mf}$ are expected to sink to the base of the bed, assuming they have a greater density.

3.8. Pressure evolution within an evolving pipe

The pressure conditions deeper in the pipe in kimberlite eruptions merit further consideration as they are relevant to processes of pipe formation and enlargement. Our analysis of explosive flows indicates that early in an eruption when the conduit is narrow the exit conditions will be pressurised with respect to the Earth's atmosphere. Such conditions are favourable for the disruption of near surface poorly consolidated deposits and rock strata, leading to the formation of a shallow explosion crater. However, at greater depth, even at this early stage of an eruption, the deeper parts of the conduit can become under-pressured. This is a consequence of the very low viscosity of the system, which results in low drag, as also recognised in the pioneering modelling study of McGetchin and Ullrich (1973).

If the pressure in the erupting mixture becomes very low in comparison to the lithostatic pressure in the wall rock or the hydrostatic pressure in the ground water system then there is the possibility of rock bursting as a consequence of widening of the conduit. Underpressures of several MPa are sufficient to exceed the tensile strength of most rocks so that rock bursting may become a major factor as the pipe widens and deepens. For saturated ground water conditions the existence of a fluid pressure should also further weaken the rocks. A plausible model for pipe widening is that at depths of 1 to 2 km under-pressuring reaches values where wall bursting initiates, creating unstable cavities and the possibility of undermining overlying rocks (Fig. 15). The widening of the conduit cross-section in the transition from the pipe to the root zone (Clement, 1982) and the formation of blind re-entrants and caverns filled with volcaniclastic kimberlite may be a consequence of this process.

3.9. Phreatomagmatism

As is the case in other varieties of volcanism it seems certain that some kimberlitic magmas will erupt in surface environments where they interact with external water such as in a lake, a river or shallow sea or in a geological setting with a large aquifer (Lorenz, 1985).

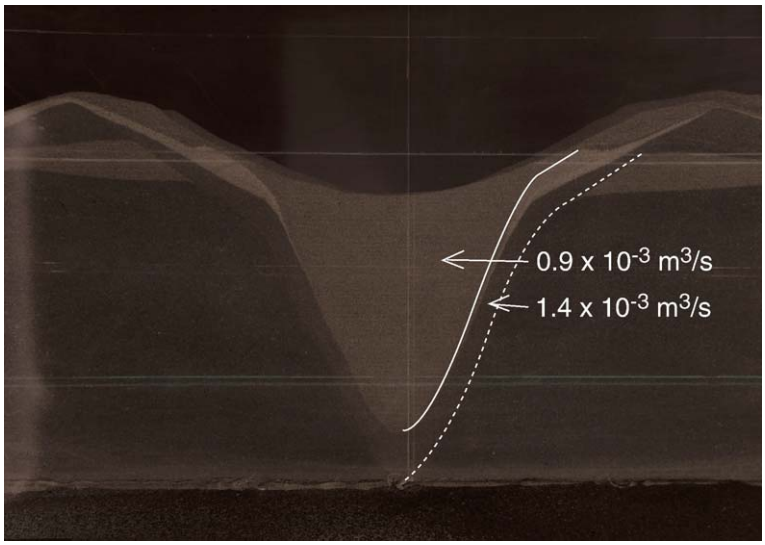

Fig. 14. Photograph of an experiment in which a two-dimensional bed of sand is fluidised by gas flowing from a narrow (8 mm) nozzle at the base of the bed. In this experiment the sand bed with markers of dark sand was first fluidised with a nozzle exit velocity of 28 m/s. This resulted in a pipe geometry of fluidised sand and rim deposits at the surface due to bursting of gas bubbles at the surface of the fluidised bed. This first fluidised structure shows slumps of marker particles from the near surface. The gas flow was turned off and the bed consolidated. When the gas flow was turned on at a lower velocity of 18 m/s another fluidised pipe formed by this pipe was narrower and so a steeply dipping internal contact was formed with the pipe fill from the first stage of the experiment.

However, a universal phreatomagmatic mechanism for kimberlitic magma is neither likely nor necessary. It would indeed be remarkable if kimberlite magmas were always by chance to erupt through parts of the crust with substantial shallow aquifers or shallow surface water. Some kimberlitic magmas erupt through low porosity crystalline basement, which provide unpromising settings for the large water flows required to sustain strong water–magma interactions.

In general as magmas rise to shallow level some interaction with ground waters is commonplace and can be a dominant feature of some volcanic eruptions. Many eruptions of more viscous magma types have phreatic and phreatomagmatic explosions for quite prolonged periods of days to months with formation of deep explosion craters that can subsequently guide magma to the surface. Examples include the early activity of Mount St Helens in 1980 (Christiansen and Peterson, 1981) and the July to November 1995 eruption of the Soufrière Hills volcano, Montserrat (Robertson et al., 2000). Such strong interaction is a consequence of slow magma ascent due to high magma viscosity and a relatively permeable fractured and porous volcanic edifice with a high water table. On the other hand there are plenty of examples of eruptions where the early involvement of external water is very brief or even negligible, such as the Hekla eruptions where relatively fluid magma rises fast and develops into a high intensity explosive eruption within a few tens of minutes of the initiation of dyke propagation from the magma chamber (Linde et al., 1993). Early phreatic interactions were also negligible in the basaltic fissure eruption of Heimaey in 1973 (Self et al., 1974) despite being on an island and along a fissure only a few hundred metres from the ocean. Strong and persistent interactions of basalt with

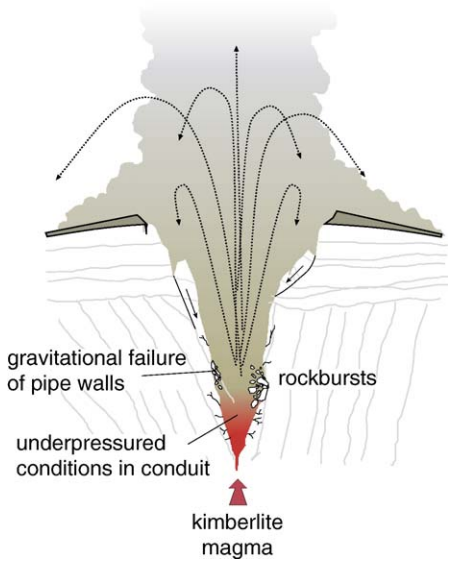

Fig. 15. Schematic of a mechanism of pipe enlargement and wall-rock erosion due to under-pressured conditions.

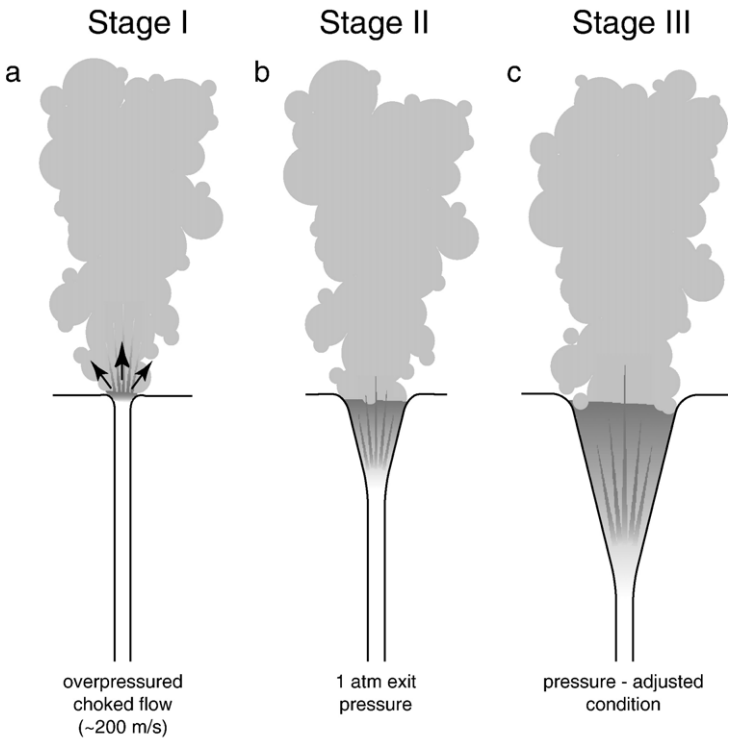

Fig. 16. Schematic depiction of a model for kimberlite eruption. The first three stages are shown with Stage IV being the post-eruption period of hydrothermal metamorphism and alteration.

ground water to form maar-type volcanoes appear to be confined to situations where there is a large near surface highly permeable aquifer, as at Ukinrek maar (Self et al., 1980). Otherwise there are innumerable examples of monogenetic cinder cone volcanoes where phreatomagmatic activity and related crater-forming explosions have not happened.

As eruptions proceed magma flows that feed lavas and domes characteristically do not revert to early phreatomagmatic activity, an observation that can be explained by drying out the aquifer in wall rocks around the conduit, sealing of fractures, for example by silica, and formation of a congealed chilled margin at the conduit margins. On the other hand phreatomagmatic eruptions can become important in explosive eruptions if the fragmentation level falls to great depths and intersects a substantial aquifer. Such a circumstance is thought to have occurred in the AD79 eruption of Vesuvius (Sheridan et al., 1981) when phreatomagmatic eruptions occurred late in the eruption as inferred from deposit characteristics.

Phreatomagmatic processes require supply of external water at rates that are comparable to or exceed magma supply rates (Wohletz, 1986; Starostin et al., 2005). Here we present some scoping calculations to show that water supply rates from saturated crystalline basement rocks around active kimberlite pipes will be small to negligible compared to magma supply rates. Consider that a large pipe that has been emptied within crystalline basement. We take conservative parameters; i.e. we choose values that tend to maximise the water flow within geologically reasonable bounds. We assume that the water table to be at the Earth's surface and give a porosity, ϕ, of 0.1 to the rocks. Consider now inflow at a depth of 1 km to a pipe of radius, r, equal to 100 m. We will further assume that the inflow occurs over a height, Z, of 500 m, on the basis that some drawdown of the water table will have occurred in forming such a substantial pipe. Darcy's law gives a water flow rate, Q_w, as follows:

$$Q_w = (2\pi r Z \phi k)(\mathrm{d}P/\mathrm{d}z)/\mu \quad (15)$$

where k is the permeability, $\mathrm{d}P/\mathrm{d}z$ is the pressure gradient and μ is the viscosity of water ($=10^{-3}$ Pa s). Manning and Ingebritsen (1999) have recently summarised estimates on the bulk permeability of continental crust. They show that in the uppermost 5 km of the crust the permeability varies between 10^{-12} and 10^{-16} m^2. This range reflects some variability in rock

types in field experiments designed to estimate bulk permeability of large volumes of crust. There is a broad tendency for permeability to decrease with depth in the shallow crust. We choose a value of 10^{-12} m^2, a value at the high end of estimates of transmissivities in country rocks around the Venetia kimberlite (Morton and Muller, 2003). We assume a pressure head of 1 km ($\sim 10^7$ Pa) over a distance of 500 m to give a pressure gradient of 2×10^4 Pa/m. The resulting flow rate is 0.6 m^3/s or 5.4×10^4 m^3/day. This scoping calculation gives a rate that is negligible compared to typical magma flow rates estimated for kimberlite eruptions. However, the flow rates are comparable to pumping rates of ground waters in active kimberlite mines and boreholes (Morton and Muller, 2003), which provide empirical estimates of long-term recharge into large open holes in continental environments. Lower permeabilities and porosities for the crustal rocks and deeper water tables would result in even smaller water flow rates.

These calculations indicate that the main circumstance where significant water magma interactions might happen as the consequence of interaction with ground waters is if a high porosity and high permeability aquifer is intersected. By increasing the pressure gradient to 10^5 Pa/s, porosity to $\phi=0.3$ and the permeability to 10^{-10} m^2, for example, a flow rate of 940 m^3/s is calculated and is well within the range of estimated magma supply rates. Strong interaction with an aquifer is most likely in the earliest phases of an eruption when pressure gradients are at their largest. High flow rates would, however, be transient and decline as draw down and draining of ground water developed; boreholes show an approximately exponential decline in flow rate as the external ground water system relaxes. This expectation is consistent with observations from many eruptions where the early phases are phreatic and phreatomagmatic, but the main activity is magmatic.

The above brief review of interactions of magma with ground water can be linked to some broad principles. Whether external water plays a role depends fundamentally on the relative supply rates of magma and ground or surface water into the conduit and on the nature of boundary zone between magma and saturated wall rocks. High magma supply rates, low permeability and low porosity wall rocks and mechanisms of sealing at or near the conduit margins can result in conditions where external water has no role. Phreatomagmatic activity can become important if magma supply rates are low, when a highly porous and permeable aquifer is intersected, which can supply a water flux at rates comparable to the magma supply rate and where there are surface bodies of water.

4. Model of kimberlite volcanism

Here we conclude by describing and discussing a general model of kimberlite eruptions (Fig. 16) based on empirical evidence, physical constraints on the nature of the magmas and the theoretical considerations developed in this paper. The eruption is divided into four stages, noting that there may in practise be overlaps between them.

4.1. Stage I: initial cratering

Two alternative viewpoints have been proposed for the early stages of kimberlite volcanism. First Lorenz (1975) proposed that interaction with near surface ground water leads to early phreatomagmatic activity and formation of a surface crater, which widens and deepens with time from the top down. Second Clement (1982) and Field and Scott Smith (1999) suggest that rising volatile-rich kimberlite magma net-veins disrupt and intrude country rock as they rise forming a disrupted zone, which is the embryonic pipe that is eventually removed when magma breaches the surface and explosive eruption begins. In this model the formation of the embryonic pipe is from the bottom to the surface, but the excavation of the pipe occurs from the near-surface downwards. Physical constraints, dynamical models and empirical evidence from modern volcanoes can help evaluate competing models and, in this case, indicate other possibilities.

Notions that dykes and sills may locally net-vein country rock and assist their weakening prior to surface eruption are plausible, but there are severe volumetric limitations in elastic rocks. There is no evidence of significant deformation, such as doming (i.e. laccolith formation), in the vicinity of kimberlite pipes, however, to create the volumes implied by the intrusive model. Strains of more than 10^{-4} are unlikely so that pre-eruptive veins, dykes, sills and dilated damaged rock can only constitute a very small proportion of the rock volume that is eventually removed to form the pipe. Thus models of intrusive mining prior to eruption have severe volume problems in cold, elastic crustal rocks and are unlikely to survive close scrutiny. However, volatiles released in advance of rising kimberlite magma may corrode and weaken crustal rocks and thus create zones of weakness that can then be exploited by kimberlite magma near the Earth's surface.

The volatile solubility and composition may be important factors in the highly explosive character of kimberlite magmas. An apparent paradox is that kimberlite magmas can form shallow dykes and sills, yet are highly explosive and lavas are so far unknown. The high solubility of water in carbonatite melts (Keppler, 2003) offers an explanation for these otherwise puzzling relationships. If kimberlite melts are water-rich and tend to towards carbonate-rich residual melts then the degassing will be very shallow but very energetic.

Here we propose that kimberlite magma reaches near the surface along narrow fissures and starts disintegrating into explosive flows within a few hundred metres of the surface. While the fissure exit remains narrow exit pressures well above atmospheric can be expected due to choked flow conditions and very quickly this will lead to explosive surface cratering to initiate the formation of the pipe. Heating and pressurisation of ground water in near surface rocks can augment magmatic explosions, as is the case in the early stages of many eruptions, but, as discussed above, it is not clear that such interactions are essential. We envisage the pipe developing from the top down (Fig. 16).

4.2. Stage II: pipe formation

As the crater widens and the pipe deepens the pressure at any given level is expected to decline because of the increase in conduit cross-sectional area. Explosive activity of sub-Plinian to Plinian intensity is able to discharge juvenile ejecta and lithic clasts derived by wall-rock failures and crater wall slumps out into the atmosphere. Widening and deepening of the conduit are postulated to accelerate as conditions are reached when the pressure difference exceeds the strength of the wall rock and rock bursts occur. Rock-bursting is expected to vary around the pipe wall due to variations in lithology, structural effects, variable stress distributions and ground water conditions. In general conditions for rock bursting will occur in the deeper parts of the developing conduit pipe (1 to 2 km) where pressure differences become comparable to rock strength. Rock bursts can lead to undermining of overlying rocks and consequent slumps of the pipe wall and inner crater wall (Fig. 14). Rock-bursts, undermining, down-faulting and crater-rim slumping widen and deepen the pipe. This is a runaway process in that, as the pipe cross-section increases and the pipe deepens, pressure differences increase as a consequence of reducing frictional resistance. Frictional resistance of magma flow is mostly controlled by the dyke at depth. As a consequence widening and deepening of the pipe will not have a large effect on magma supply rate. However the near surface explosive flows and distribution of pressure will be strongly affected, as is clear from numerical models of explosive flows in conduits (Woods, 1995; Sparks et al., 1997; Papale, 1999). Stage II represents a largely erosive stage when the pipe is formed.

There is evidence in some kimberlites that the pipes were sometimes empty allowing failed crater wall and pipe margins to fall down into the deep interior of the pipe. Some pipes, such as the Ekati, Diavik and Lac de Gras pipes in Northwest Territory, Canada and Jwaneng in Botswana, preserve wood and breccias composed of rocks or sediments from near or at the surface. Such pipes may represent cases where the eruption came to a stop while the pipe was still largely empty and then became infilled by post-eruption erosion and possibly by infilling from later nearby kimberlite eruptions.

4.3. Stage III: pipe filling

We have identified in calculations (Fig. 12) a significant change when the exit conditions are such that the erupting mixture can reach one atmosphere. Beyond this threshold further pipe widening and deepening associated with increasing under-pressures, the gas velocities decline rapidly with increasing cross-sectional area (Fig. 12a) and ability for the flows to clear material from the conduit also declines markedly (Fig. 12b). Crater walls and pipe margins collapse but large blocks can no longer be removed unless they are broken down. Thus Stage III can be defined as the stage in which the pipe starts to infill. Breccias and layered volcaniclastic kimberlite are commonly preserved at the outer margins of kimberlite pipes. Such marginal facies are formed in the transition between stages II and III when the activity is no longer able to empty out the entire pipe following episodes of wall-rock failure and crater wall slumping.

The transition from pipe formation to pipe-infilling need not occur exactly at the dynamical threshold. As the pipe widens and deepens further into the pressure-adjusted regime (Fig. 12) eruptive activity is increasingly confined within the pipe and conditions develop where pyroclastic materials can be trapped. Three main factors can contribute to the onset of pipe-filling. First the increase in cross-sectional area of the pipe must decrease the vertical speed at any given level for fixed pressure and supply rate. The system transforms to one where atmospheric pressure will be reached below surface and vertical gas speeds are unable to transport

coarse clasts out of the pipe. Second if the magma supply rate declines the explosive intensity decreases and there is more opportunity for gas bubbles to segregate non-explosively from rising low viscosity melt. Third as coarse clasts become trapped in the pipe a fluidised bed starts to fill up the pipe and further suppresses explosive activity from input of new magma. The fluidised bed provides a major barrier and only gas and fines can escape through it. This fluidised bed is fed by further wall-rock bursts and slumps and by strongly degassing new magma fed into its base. Gas fluidisation in the diverging pipe geometry results in thorough mixing of the trapped particles (see Walters et al., 2005 for more detail). It evolves into the VK fill. Ultimately magma supply rates become so low that rising magma loses its gas passively by bubbling and so late stage dykes and sills can be intruded into pipe fill. Late stage welding processes at the base of the pipe can also form massive and irregular magmatic kimberlite facies.

The transition between stages II and III is not envisaged as a simple two-stage sequence with an abrupt transition. Rather we envisage that there are alternating and overlapping episodes of pipe enlargement, emptying and filling. The tendency with time will be for the system to evolve from largely pipe erosion with explosive flows able to clear the conduit of ejecta to pipe-filling as the pipe enlarges and explosive activity wanes. The internal geology of most kimberlites indeed indicates large fluctuations in activity with complex internal cross-cutting contacts between different volcaniclastic kimberlite units and breccias. These fluctuations might have a deep causation due to pulses of kimberlite magma ascent from depth. Alternatively they could arise by modulation of the near surface flows due to, for example, temporary blocking of the conduit by wall-rock slumps and build up of pressure in magma trapped beneath a blockage.

4.4. Stage IV: post-emplacement metamorphism and alteration

The final stage occurs after eruption with the emplacement of hot volcaniclastic deposits in the pipe. Bodies of tens to hundreds of metres in width are expected to take decades to many centuries to cool down by conduction. Circulation of meteoric water through the hot pipe fill results in hydrothermal metamorphism with serpentinisation being the principal consequence. Evidence that the fluid phase is largely meteoric water rather than magmatic gases comes from the low CO_2 contents and sub-solidus temperatures calculated for the fluid that can form the common mineral assemblages (Fig. 8). Serpentinisation of olivine involves large volume changes and as a consequence original primary pore space in the volcaniclastic deposits is infilled with products of hydrothermal metamorphism, principally serpentinisation. Metamorphism merges into low temperature alteration as the kimberlite bodies equilibrate thermally with their surroundings.

5. Final remarks

This paper has attempted to integrate geological and petrological observations on kimberlites with current understanding of volcanic processes, dynamical constraints and experimental data. The proposed model is no more than a series of working hypotheses. It is clear that there are large areas of uncertainty in understanding the nature of kimberlite magmas and considerable difficulties in interpreting the geology. There remains a great deal of research to do.

Acknowledgements

The support of De Beers MRM R and D Group through the auspices of the Diamond Trading Company is much appreciated. Many De Beers geologists and petrologists have been very generous with their time and information during field trips to southern Africa and Canada for the purpose of familiarising the first author with kimberlite geology; RSJS thanks Wayne Barnett, Roger Mitchell, Barbara Scott Smith, Casey Hetman, Jock Robey and Kimberley Webb in particular. RSJS also acknowledges a Royal Society–Wolfson Merit Award. Thanks go to Don Dingwell for helpful discussions about estimates of viscosity of kimberlite melts and to Anton Le Roux over discussions concerning kimberlite melt compositions. Reviews by Marcus Bursik and Barbara Scott Smith and discussions with Ray Cas are acknowledged.

References

Alidibirov, M.A., Dingwell, D.B., 1996. Magma fragmentation by rapid decompression. Nature 380, 146–148.

Armstrong, J.P., Wilson, M., Barnett, R.L., Nowicki, T., Kjarsgaard, B. A., 2004. Mineralogy of primary carbonate-bearing hypabyssal kimberlite, Lac de Gras, Slave Province, Northwest Territories, Canada. Lithos 76, 415–433.

Atkinson, B.K., 1994. Subcritical crack growth in geological materials. Journal of Geophysical Research 89, 4077–4114.

Audetat, A., Keppler, H., 2004. Viscosity of fluids in subduction zones. Science 303, 513–516.

Bailey, D.K., 1980. Volatile flux, geotherms, and the generation of the kimberlite–carbonatite–alkaline magma spectrum. Mineralogical Magazine 43, 695–699.

Bailey, D.K., 1984. Kimberlite: the mantle sample formed by ultrametamorphism. In: Kornprobst, J. (Ed.), Kimberlites and Related Rocks, pp. 323–333.

Barnett, W.P., 2004. Subsidence breccias in kimberlite pipes: an application of fractal analysis. Lithos 76, 299–316.

Blank, J.G., Brooker, R.A., 1994. Experimental studies of carbon dioxide in silicate melts: solubility, speciation and stable isotope behaviour. Volatiles in Magmas. Reviews in Mineralogy, vol. 30, pp. 157–186.

Boyd, F.R., Nixon, P.H., 1975. Origins of the ultramafic nodules from some kimberlites of northern Lesotho and the Monastery Mine, South Africa. Physics and Chemistry of the Earth 9, 431–453.

Brey, G.P., Ryabchikov, I.D., 1994. Carbon dioxide in strongly silica undersaturated melts: an origin for kimberlite magmas. Neues Jahrbuch fur Mineralogie Monatshefte 10, 449–463.

Brooker, R.A., Kohn, S., Holloway, J.R., McMillan, P.F., 2001. Structural controls on the solubility of CO_2 in silicate melts: Part I. Bulk solubility data. Chemical Geology 174, 225–239.

Canil, D., Fedortchouk, Y., 1999. Garnet dissolution and the emplacement of kimberlites. Earth and Planetary Science Letters 167, 227–237.

Cas, R.A.F., Wright, J.V., 1987. Volcanic Successions, Modern and Ancient. Chapman and Hall, London.

Christiansen, R.L., Peterson, D.W., 1981. Chronology of the 1980 eruptive activity. U.S. Geological Survey Special Paper 1250, 17–30.

Clavero, J., Sparks, R.S.J., Huppert, H.E., Dade, W.B., 2002. Geological constraints on the emplacement mechanism of the Parinacota debris avalanche, northern Chile. Bulletin of Volcanology 64, 3–20.

Clement, C.R., 1975. The emplacement of some diatreme facies kimberlites. Physics and Chemistry of the Earth 9, 51–59.

Clement, C.R., 1979. The origin and infilling of kimberlite pipes. Kimberlite Symposium II. Cambridge. Extended abstract.

Clement, C.R., 1982. A comparative geological study of some major kimberlite pipes in northern Cape and Orange Free State. PhD thesis (unpublished) University of Cape Town, p. 432.

Clement, C.R., Reid, A.M., 1989. The origin of kimberlite pipes: an interpretation based on the synthesis of geological features displayed by southern African occurrences. In: Ross, J., Jaques, A.L., Fergusan, J., Green, D.H., O'Reilly, S.Y., Danchin, R.V., Janse, A.J.A. (Eds.), Kimberlites and Related Rocks, vol. 14. Geological Society of Australia, Sydney, pp. 632–646.

Cloos, H., 1941. Bau und Takgkeit von Tuffscholten. Geologische Rundschau 32, 709–800.

Connolly, J.A.D., 1990. Multivariable phase-diagrams — an algorithm based on generalized thermodynamics. American Journal of Science 290, 666–718.

Dalton, J.A., Presnall, D.C., 1998a. The continuum of primary carbonatitic-kimberlite melt compositions in equilibrium with lherzolite: data from the system $CaO–MgO–Al_2O_3–SiO_2–CO_2$ at 6 GPa. Journal of Petrology 39, 1953–1964.

Dalton, J.A., Presnall, D.C., 1998b. Carbonatitic melts along the solidus of model lherzolite in the system $CaO–MgO–Al_2O_3–SiO_2–CO_2$ from 3 to 7 GPa. Contributions to Mineralogy and Petrology 131, 123–135.

Dawson, J.B., 1971. Advances in kimberlite geology. Earth Science Reviews 7, 187–214.

Dawson, J.B., 1973. Baustoland kimberlites. Bulletin of the Geological Society of America 73, 545–560.

Dawson, J.B., Hawthorne, J.B., 1973. Magmatic sedimentation and carbonatitic differentiation in kimberlite sills at Benfontein, South Africa. Journal of Geological Society London 129, 61–85.

Dingwell, D.B., Courtial, P., Giordano, D., Nichols, A.R.L., 2004. Viscosity of peridotite liquid. Earth and Planetary Science Letters 226, 127–138.

Edgar, A.D., Arima, M., Baldwin, D.K., Bell, D.R., Shee, S.R., Skinner, E.M.W., Walker, E.C., 1988. High-pressure–high temperature melting experiment on a SiO_2-poor aphanitic kimberlite from the Wesselton mine, Kimberley, South Africa. American Mineralogist 73, 524–533.

Eggler, D.H., 1978. The stability of dolomite in a hydrous mantle, with implications for the mantle solidus. Geology 6, 397–400.

Ekkerd, J., Stienhofer, J., Field, M., Lawless, P.J., 2003. The geology of the Finsch Mine, Northern Cape Province, South Africa. 8th International Kimberlite Conference. Extended abstract.

Evans, B.W., 1977. Metamorphism of Alpine peridotites and serpentine. Annual Reviews of Earth and Planetary Science 5, 397–447.

Evans, B.W., 2004. The serpentine multisystem revisited: chrysotile is metastable. International Geology Review 46, 479–506.

Ferguson, J., Danchin, R.V., Nixon, P.H., 1975. Petrochemistry of kimberlite autoliths. Lesotho 285–293.

Field, M., Scott Smith, B.H., 1998. Textural and genetic classification schemes for kimberlites: a new perspective. Proceedings of the VIIth International Kimberlite Conference, vol. 1, pp. 214–216.

Field, M., Scott Smith, B.H., 1999. Contrasting geology and near-surface emplacement of kimberlite pipes in southern Africa and Canada. Proceedings of the VIIth International Kimberlite Conference, vol. 1, pp. 217–237.

Field, M., Gibson, J.G., Wikes, T.A., Gababotse, J., Khutjwe, P., 1997. The geology of the Orapa A/K1 kimberlite Botswana: further insight into the emplacement of kimberlite pipes. Russian Geology and Geophysics 38, 24–39.

Fisher, R.V., 1961. Proposed classification scheme of volcaniclastic sediments and rocks. Geological Society of America Bulletin 72, 1409–1414.

Fisher, R.V., Schmincke, H.U., 1984. Pyroclastic Rocks. Springer Verlag, Berlin. 472 pp.

Francis, P.W., Gardeweg, M., Ramirez, C.F., Rothery, D.A., 1985. Catastrophic debris avalanche deposit of Socompa volcano, northern Chile. Geology 13, 600–603.

Franz, L., Brey, G.P., Okrusch, M., 1996. Re-equilibrium of ultramafic xenoliths from Namibia by metasomatic processes at the mantle boundary. Journal of Geology 104, 599–615.

Glicken, H., 1998. Rock-slide debris avalanche of May 18 1980, Mount St Helens volcano, Washington. Bulletin of the Geological Society of Japan 49, 55–106.

Golovin, A.V., Sharygin, V.V., Pokhilenko, N.P., Mal'kovets, V.G., Sobolev, N.K., 2003. Secondary melt inclusions in olivine from unaltered kimberlites of the Udachnaya-eastern pipe, Yakutia. Proceedings of the 8th International Kimberlite, pp. 1–5.

Gurney, J.J., Helmstaedt, H., Moore, R.O., 1993. A review of the use and application of mantle mineral geochemistry in diamond exploration. Pure and Applied Chemistry 65, 2423–2442.

Haggerty, S.E., 1994. Superkimberlites: a geodynamic diamond window to the earth's core. Earth and Planetary Science Letters 122, 57–59.

Harris, M., Le Roex, A., Class, C., 2004. Geochemistry of the Unitjiesberg kimberlite, South Africa: petrogenesis of an off-craton, group 1, kimberlite. Lithos 74, 149–165.

Hawthorne, J.B., 1975. Model of a kimberlite pipe. Physics and Chemistry of the Earth 9, 1–15.

Hetman, C.M., Scott-Smith, B.H., Paul, J.L., Winter, F., 2004. Geology of the Gahcho Kue kimberlite pipes, NWT, Canada: root to diatreme magmatic transition zone. Lithos 76, 51–74.

Holland, T.J.B., Powell, R., 1998. An internally consistent thermodynamic data set for phases of petrological interest. Journal of Metamorphic Geology 16, 309–343.

Huppert, H.E., Sparks, R.S.J., 1985a. Komatiites I: eruption and flow. Journal of Petrology 26, 694–725.

Huppert, H.E., Sparks, R.S.J., 1985b. Cooling and contamination of mafic and ultramafic magmas during ascent through continental crust. Earth and Planetary Science Letters 74, 371–386.

Hyndman, R.D., Peacock, S.M., 2003. Serpentinization of the forearc mantle. Earth and Planetary Science Letters 212, 417–432.

Kaminsky, F.V., Feldman, A.A., Varlamov, V.A., Boyko, A.N., Olofinsky, L.N., Shofman, I.L., Vaganov, V.I., 1995. Prognostication of primary diamond deposits. In: Griffin, W.L. (Ed.), Diamond Exploration into the 21st Century. Journal of Geochemical Exploration, vol. 53, pp. 167–182.

Kelley, S.P., Wartho, J.A., 2000. Rapid kimberlite ascent and the significance of Ar–Ar ages in xenoliths phlogopites. Science 289, 609–611.

Keppler, H., 2003. Water solubility in carbonate melts. American Mineralogist 88, 1822–1824.

Kjarsgaard, B.A., 1996. Kimberlite-hosted diamond. In: Eckstrand, O.R., Sinclair, W.D., Thorpe, R.I. (Eds.), Geology of Canadian Mineral Deposit Types. Geological Survey of Canada, vol. 8, pp. 560–568.

Kurszlaukis, S., Barnett, W.P., 2003. Volcanological and structural aspects of the Venetia kimberlite cluster — a case study of South African kimberlite maar–diatreme volcanoes. South African Journal of Geology 106, 165–192.

Kurszlaukis, S., Büttner, R., Zimanowski, B., Lorenz, V., 1998. On the first experimental phreatomagmatic explosion of a kimberlite melt. Journal of Volcanology and Geothermal Research 80, 323–326.

Le Roux, A.P., Bell, D.R., Davis, P., 2003. Petrogenesis of Group I kimberlites from Kimberley, South Africa: evidence from bulk rock geochemistry. Journal of Petrology 44, 2261–2286.

Lee, W.J., Haung, W.L., Wyllie, P.J., 2000. Melts in the mantle modeled in the system SiO_2–MgO–CaO–CO_2 at 2.7 GPa. Contributions to Mineralogy and Petrology 138, 199–213.

Linde, A.Y., Augustsson, K., Sacks, I.S., Stefansson, R., 1993. Mechanisms of the 1991 eruption of Hekla from continuous borehole strain monitoring. Nature 365, 737–740.

Lister, J.R., Kerr, R.C., 1991. Fluid-mechanical models of crack propagation and their application to magma transport in dykes. Journal of Geophysical Research 96, 10049–10077.

Lorenz, V., 1975. Formation of phreatomagmatic maar–diatreme volcanoes and its relevance to kimberlite diatremes. Physics and Chemistry of the Earth 9, 17–29.

Lorenz, V., 1985. Maars and diatremes of phreatomagmatic origin. Transactions of the Geological Society of South Africa 88, 459–470.

Lorenz, V., Zimanowski, B., Büttner, R., Kurszlaukis, S., 1998. Formation of kimberlite diatremes by explosive interaction of kimberlite magma with groundwater: field and experimental aspects. Proceedings of the VIIth International Kimberlite Conference, vol. 2, pp. 522–528.

Manning, C.E., Ingebritsen, S.E., 1999. Permeability of the continental crust: implications of thermal data and metamorphic systems. Reviews of Geophysics 37, 127–150.

McGetchin, T.R., 1968. The Moses Rock dyke: geology, petrology and mode of emplacement of kimberlite-bearing breccia, San Juan County, Utah. PhD Thesis Caltech.

McGetchin, T.R., Ullrich, G.W., 1973. Xenoliths in maars and diatremes, with references for the moon, Mars and Venus. Journal of Geophysical Research 78, 1832–1852.

Melnik, O., Sparks, R.S.J., 2002. Modelling of conduit flow dynamics during explosive activity at Soufrière Hills Volcano, Montserrat. In: Druitt, T.H., Kokelaar, B.P. (Eds.), The Eruption of the Soufrière Hills Volcano, Montserrat 1995 to 1999. Geological Society of London, Memoir, vol. 21, pp. 307–318.

Menand, T., Tait, S.R., 2002. The propagation of a buoyant liquid-filled fissure from a source under constant pressure: an experimental approach. Journal of Geophysical Research 107, 2306 (16-1-14).

Mitchell, R.H., 1984. Mineralogy and origin of carbonate-rich segregations in a composite kimberlite sill. Neues Jahrbuch fur Mineralogie. Abhandlungen 150, 185–197.

Mitchell, R.H., 1986. Kimberlites: Mineralogy, Geochemistry and Petrology. Plenum Press, NY, p. 442.

Mitchell, R.H., 1997. Kimberlites, Orangeites, Lamproites, Melitites, and Minettes: A Petrological Atlas. Ontario Almaz Press, Thunder Bay, p. 243.

Moore, R.O., Gurney, J.J., 1985. Pyroxene solid solution in garnets included in diamond. Nature 318, 553–555.

Morton, K.L., Muller, S., 2003. Hydrogeology of the Venetia Diamond Mine, South Africa. South African Journal of Geology 106, 193–204.

Moore, K.R., Wood, B.J., 1998. The transition from carbonate to silicate melts in the CaO–MgO–SiO_2–CO_2 system. Journal of Petrology 39, 1943–1951.

Naidoo, P., Stefenhofer, J., Field, M., Dobbe, R., 2004. Recent advances in the geology of Koffiefontein Mine, Free State Province, South Africa. Lithos 76, 161–182.

Palandri, J.L., Reed, M.H., 2004. Geochemical models of metasomatism in ultramafic systems: serpentinization, rodingization and sea-floor carbonate precipitation. Geochimica et Cosmochimica Acta 68, 1115–1133.

Papale, P., 1999. Strain-induced magma fragmentation in explosive eruptions. Nature 397, 425–428.

Pinkerton, H., Stevenson, R., 1992. Methods of determining the rheological properties of magmas at sub-liquidus temperatures. Journal of Volcanology and Geothermal Research 53, 47–88.

Phillips, D., Harris, J., 2003. The effect of differential mineral compressibility of diamond inclusion geobarometry. Abstract: 8th International Kimberlite Conference, Victoria BC, Canada.

Price, S.E., Russell, J.K., Koplova, M.G., 2000. Primitive magma from the Jericho Pipe, NWT, Canada: constraints on primary kimberlite melt chemistry. Journal of Petrology 41, 789–808.

Priestley, K., McKenzie, D., Debayle, E., in press. The state of the upper mantle beneath southern Africa. Physics and Chemistry of the Earths Interior.

Reedman, A.J., Park, K.H., Merriman, R.J., Kim, S.E., 1987. Welded tuff infilling a volcanic vent at Weolseong, Republic of Korea. Bulletin of Volcanology 49, 541–546.

Reches, Z., Fink, J., 1988. The mechanism of intrusion of the Inyo Dike, Long Valley, California. Journal of Geophysical Research 93, 4321–4334.

Reid, A.H., Donaldson, C.H., Dawson, J.B., Brown, W.R., Ridley, W.I., 1975. The Igwisi Hills extrusive kimberlite. Physics and Chemistry of the Earths Interior 9, 199–223.

Riedel, C., Ernst, G.G.J., Riley, M., 2003. Controls on the growth and geometry of pyroclastic constructs. Journal of Volcanology and Geothermal Research 127, 1–33.

Ringwood, A.E., Kesson, S.E., Hibberson, W., Ware, N., 1992. Origin of kimberlites and related magmas. Earth and Planetary Science Letters 113, 521–538.

Robertson, R.E.A., Aspinall, W.P., Herd, R.A., Norton, G.E., Sparks, R.S.J., Young, S.R., 2000. The 1995–98 eruption of the Soufriere Hills volcano, Montserrat. Philosophical Transactions of the Royal Society 358, 1619–1637.

Rubin, A.M., 1995. Propagation of magma-filled cracks. Annual Reviews of Earth and Planetary Science 23, 287–336.

Schmincke, H.U., 1974. Volcanological aspects of peralkaline silicic welded ash-flow tuffs. Bulletin of Volcanology 38, 594–636.

Scholtz, C.H., Dawers, N.H., Yu, J.-Z., Anders, M.H., Cowie, P.A., 1993. Fault growth and fault scaling laws; preliminary results. Journal of Geophysical Research 98, 21951–21961.

Self, S., Kienle, J., Huot, J.P., 1980. Ukinrek maars, Alaska: II. Deposits and formation of the 1977 craters. Journal of Volcanology and Geothermal Research 7, 39–65.

Self, S., Sparks, R.S.J., Booth, B., Walker, G.P.L., 1974. The 1973 Heimaey Strombolian scoria deposit. Geological Magazine 111, 539–548.

Sheppard, S.M.F., Dawson, J.B., 1975. Hydrogen, carbon, and oxygen isotope studies of megacryst and matrix minerals from Lesothan and South African kimberlites. Physics and Chemistry of the Earth 9, 747–763.

Sheridan, M.F., Barberi, F., Rosi, M., Santacroce, R., 1981. A model for Plinian eruptions at Vesuvius. Nature 282, 24–28.

Skinner, E.M.W., 1989. Contrasting Group 1 and Group 2 kimberlite petrology: towards a genetic model of kimberlites. In: Ross, J., Jaques, A.L., Fergusan, J., Green, D.H., O'Reilly, S.Y., Danchin, R.V., Janse, A.J.A. (Eds.), Kimberlites and Related Rocks, vol. 14. Geological Society of Australia, Sydney, pp. 528–544.

Skinner, E.M.W., Clement, C.R., 1979. Mineralogical classification of southern African kimberlites. In: Boyd, F.R., Meyer, H.O.A. (Eds.), Proceedings of 2nd International Kimberlite Conference, Washington D.C. AGU, pp. 129–139.

Skinner, E.M.W., Marsh, J.S., 2004. Distinct kimberlite classes with contrasting eruption processes. Lithos 76, 183–200.

Smith, R.L., 1960. Zones and zonal variations in welded ash flows. US Geological Survey Professional Paper 354-F, 149–159.

Snyder, D.B., Lockhart, G.D., 2005. Kimberlite trends in NW Canada. Journal of the Geological Society of London 162, 737–740.

Sosman, R.B., 1938. Evidence on the intrusion-temperature of peridotites. American Journal of Science 35, 353–359.

Sparks, R.S.J., 1976. Grain size variations in ignimbrites and implications for the transport of pyroclastic flows. Sedimentology 23, 147–188.

Sparks, R.S.J., 1988. The petrology and geochemistry of the Loch Ba ring-dyke, Mull (N.W. Scotland): implications for the extreme (Skaergaard-type) differentiation of tholeiitic magmas. Contributions to Mineralogy and Petrology 100, 446–461.

Sparks, R.S.J., 2003. Dynamics of degassing. In: Oppenheimer, C., Pyle, D.M., Barclay, J. (Eds.), Volcanic Degassing. Geological Society of London Special Publication, vol. 213, pp. 5–22.

Sparks, R.S.J., Bursik, M.I., Carey, S.N., Gilbert, J.S., Glaze, L., Sigurdsson, H., Woods, A.W., 1997. Volcanic Plumes. John Wiley and Sons, p. 557.

Spera, F.J., 1984. Carbon dioxide in igneous petrogenesis III: role of volatiles in the ascent of alkaline magma with special reference to xenolith-bearing mafic lavas. Contributions to Mineralogy and Petrology 88, 217–232.

Starostin, A.B., Melnik, O.E., Barmin, A.A., 2005. A transient model for explosive and phreatomagmatic eruptions. Journal of Volcanology and Geothermal Research 143, 133–151.

Stasiuk, M.V., Jaupart, C., Sparks, R.S.J., 1993. Variations of flow rate and volume during eruption of lava. Earth and Planetary Science Letters 114, 505–516.

Stasiuk, L.D., Lockhart, G.D., Nassichuk, W.W., 1999. Thermal maturity evaluation of dispersed organic matter inclusions from kimberlite pipes, Lac de Gras, Northwest Territories, Canada. International Journal of Coal Geology 40, 1–25.

Stebbins, J.F., Carmichael, I.S.E., 1984. The heat of fusion of fayalite. American Mineralogist 69, 292–297.

Stebbins, J.F., Carmichael, I.S.E., Weill, D.E., 1983. The high temperature liquid and glass heat contents and the heats of fusion of diopside, albite, sanidine and nepheline. American Mineralogist 68, 717–730.

Stiefenhofer, J., Farrow, D.J., 2004. Geology of the Mwadui kimberlite, Shinyanga district, Tanzania. Lithos 76, 139–160.

Sumner, J.M., 1998. Formation of clastogenic lava flow during fissure eruption and scoria cone collapse: the 1996 eruption of Izu-Oshima, eastern Japan. Bulletin of Volcanology 60, 195–212.

Tainton, K., McKenzie, D., 1994. The generation of kimberlites, lamproites and their source rocks. Journal of Petrology 35, 787–817.

Tappert, R., Stachel, T., Harris, J.W., Muehlenbachs, K., Ludwig, T., Brey, G.P., 2005. Subducting oceanic lithosphere: the source of deep diamonds. Geology 33, 565–568.

Tuffen, H., Gilbert, J., McGarvie, D., 2001. Products of an effusive subglacial rhyolite eruption: Blahnukar, Torfajokull, Iceland. Bulletin of Volcanology 63, 179–190.

Tuffen, H., Dingwell, D.B., Pinkerton, H., 2003. Repeated fracture and healing of silicic magma generate flow-banding and earthquakes? Geology 31, 1089–1092.

Voight, B., Komorowski, J.-C., Norton, G.E., Belousov, A.B., Belousova, M., Boudon, G., Francis, P.W., Franz, W., Heinrich, P., Sparks, R.S.J., Young, S.R., 2002. The 26 December (Boxing Day) 1997 sector collapse and debris avalanche at Soufrière Hills Volcano, Montserrat. In: Druitt, T.H., Kokelaar, B.P. (Eds.), The Eruption of Soufrière Hills Volcano, Montserrat, from 1995 to 1999. Geological Society of London Memoir, vol. 21, pp. 363–408.

Walters, A., Phillips, J., Brown, R., Field, M., Sparks, R.S.J., 2006. The role of fluidisation processes in the formation of volcaniclastic kimberlite: grain size observations and experimental investigation. Journal of Volcanology and Geothermal Research. 155, 119–137 (this volume).

Watson, K.D., 1967. Kimberlites of eastern North America. In: Wiley, P.J. (Ed.), Ultramafic and Related Rocks, pp. 312–323.

Webb, K.J., Scott-Smith, B.H., Paul, J.L., Hetman, C.M., 2004. Geology of the Victor kimberlite, Attawapiskat, northern Ontario, Canada: cross-cutting and nested craters. Lithos 76, 29–50.

Wilson, L., 1976. Explosive volcanic eruptions III. Plinian eruption columns. Geophysical Journal of the Royal Astronomical Society 45, 543–556.

Wilson, C.J.N., 1984. The role of fluidization in the emplacement of pyroclastic flows: 2. Experimental results and their interpretation. Journal of Volcanology and Geothermal Research 20, 55–84.

Wilson, L., Head, J.W., 1981. Ascent and eruption of basaltic magma on the earth and moon. Journal of Geophysical Research 86, 2971–3001.

Wohletz, K., 1986. Explosive magma–water interactions; thermodynamics, explosion mechanisms, and field studies. Bulletin of Volcanology 48, 245–264.

Woods, A.W., 1995. The dynamics of explosive volcanic eruptions. Reviews of Geophysics 33, 495–530.

Woolsey, T.S., McCallum, M.E., Schumm, S.A., 1975. Modelling of diatreme emplacement by fluidization. Physics and Chemistry of the Earths Interior 9, 30–42.

Wyllie, P.J., 1980. The origin of kimberlite. Journal of Geophysical Research 85, 6902–6910.

Wyllie, P.J., Tuttle, O.F., 1960. The system $CaO–CO_2–H_2O$ and the origin of carbonatites. Journal of Petrology 1, 1–46.